

AD-A038 292

COLD REGIONS RESEARCH AND ENGINEERING LAB HANOVER N H
RADIOSOUNDING OF ICE (RADIOZONDIROVANIYE L'DA), (U)

F/G 8/12

APR 77 V V BOGORODSKIY

UNCLASSIFIED

CRREL-TL-614

NL

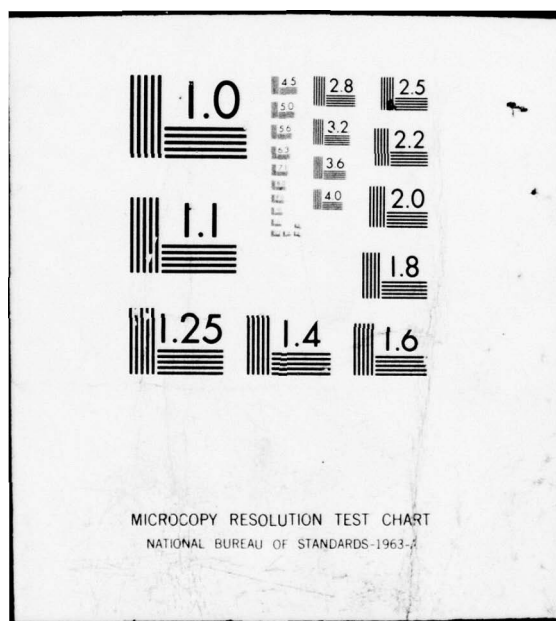
1 OF /
AD
A038 292



END

DATE
FILMED

5 - 77



TL 614



ADA 038292

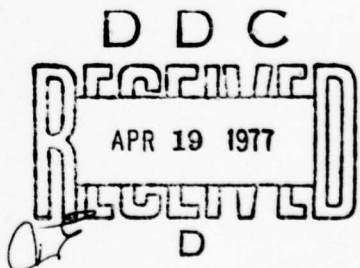
Draft Translation 614
April 1977

RADIOSOUNDING OF ICE

V.V. Bogorodskiy

AD No. _____
DDC FILE COPY
DDC

CORPS OF ENGINEERS, U.S. ARMY
COLD REGIONS RESEARCH AND ENGINEERING LABORATORY
HANOVER, NEW HAMPSHIRE



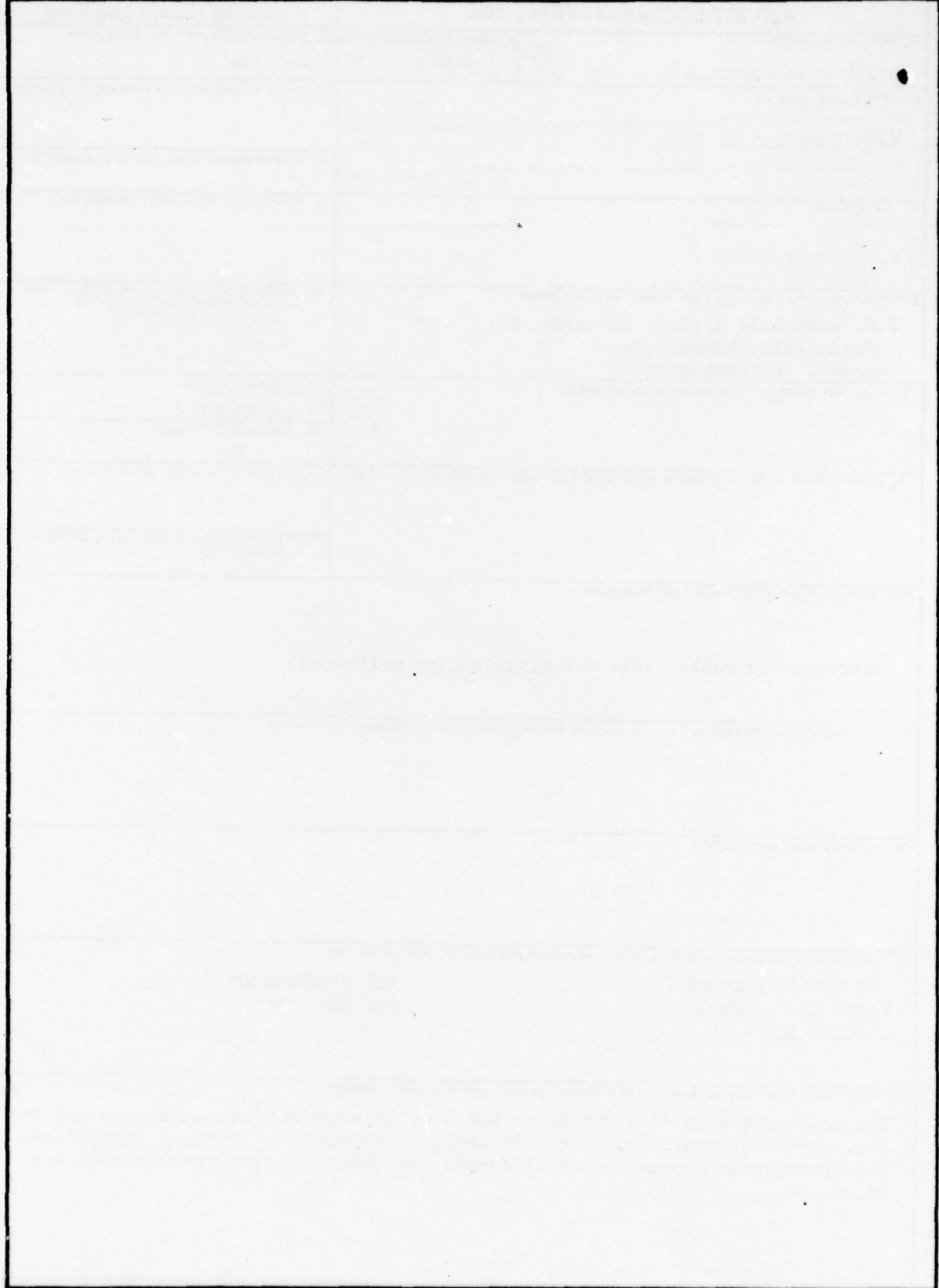
Approved for public release; distribution unlimited.

Unclassified

SECURITY CLASSIFICATION OF THIS PAGE (When Data Entered)

REPORT DOCUMENTATION PAGE		READ INSTRUCTIONS BEFORE COMPLETING FORM
1. REPORT NUMBER	2. GOVT ACCESSION NO.	3. RECIPIENT'S CATALOG NUMBER
Draft Translation 614	(14) CRREL-TL-614	
4. TITLE (and Subtitle)	5. TYPE OF REPORT & PERIOD COVERED	
(6) RADIOSOUNDING OF ICE, (Radiozondirovaniye L'da),		
7. AUTHOR(s)	6. PERFORMING ORG. REPORT NUMBER	
(10) V.V. Bogorodskiy	8. CONTRACT OR GRANT NUMBER(s)	
9. PERFORMING ORGANIZATION NAME AND ADDRESS	10. PROGRAM ELEMENT, PROJECT, TASK AREA & WORK UNIT NUMBERS	
U.S. Army Cold Regions Research and Engineering Laboratory Hanover, New Hampshire	(12) 86P.	
11. CONTROLLING OFFICE NAME AND ADDRESS	12. REPORT DATE	
	(11) April 1977	
14. MONITORING AGENCY NAME & ADDRESS (if different from Controlling Office)	13. NUMBER OF PAGES	
	83	
16. DISTRIBUTION STATEMENT (of this Report)	15. SECURITY CLASS. (of this report)	
Approved for public release; distribution unlimited.		
17. DISTRIBUTION STATEMENT (of the abstract entered in Block 20, if different from Report)		
18. SUPPLEMENTARY NOTES		
19. KEY WORDS (Continue on reverse side if necessary and identify by block number)		
ICE COVER THICKNESS RADIO ECHO SOUNDING GLACIER ICE	ICE DIELECTRICS SEA ICE	
20. ABSTRACT (Continue on reverse side if necessary and identify by block number)		
The pulse radiosounding technique was used in studying Antarctic land and sea ice, their internal structures, volumes, movements, and physical properties. Electromagnetic properties of different ice types and their measurement are discussed.		

SECURITY CLASSIFICATION OF THIS PAGE(When Data Entered)



SECURITY CLASSIFICATION OF THIS PAGE(When Data Entered)

DRAFT TRANSLATION 614

1	White Section	<input checked="" type="checkbox"/>
2	Buff Section	<input type="checkbox"/>
3	Classification	<input type="checkbox"/>
4	Security Mark	<input type="checkbox"/>
5		
TRANSLATION/AVAILABILITY CODES		
6		
7 AVAIL. and/or SPECIAL		
8		
9		
10		
11		
12		
13		
14		
15		
16		
17		
18		
19		
20		
21		
22		
23		
24		
25		
26		
27		
28		
29		
30		
31		
32		
33		
34		
35		
36		
37		
38		
39		
40		
41		
42		
43		
44		
45		
46		
47		
48		
49		
50		
51		
52		
53		
54		
55		
56		
57		
58		
59		
60		
61		
62		
63		
64		
65		
66		
67		
68		
69		
70		
71		
72		
73		
74		
75		
76		
77		
78		
79		
80		
81		
82		
83		
84		
85		
86		
87		
88		
89		
90		
91		
92		
93		
94		
95		
96		
97		
98		
99		
100		
101		
102		
103		
104		
105		
106		
107		
108		
109		
110		
111		
112		
113		
114		
115		
116		
117		
118		
119		
120		
121		
122		
123		
124		
125		
126		
127		
128		
129		
130		
131		
132		
133		
134		
135		
136		
137		
138		
139		
140		
141		
142		
143		
144		
145		
146		
147		
148		
149		
150		
151		
152		
153		
154		
155		
156		
157		
158		
159		
160		
161		
162		
163		
164		
165		
166		
167		
168		
169		
170		
171		
172		
173		
174		
175		
176		
177		
178		
179		
180		
181		
182		
183		
184		
185		
186		
187		
188		
189		
190		
191		
192		
193		
194		
195		
196		
197		
198		
199		
200		
201		
202		
203		
204		
205		
206		
207		
208		
209		
210		
211		
212		
213		
214		
215		
216		
217		
218		
219		
220		
221		
222		
223		
224		
225		
226		
227		
228		
229		
230		
231		
232		
233		
234		
235		
236		
237		
238		
239		
240		
241		
242		
243		
244		
245		
246		
247		
248		
249		
250		
251		
252		
253		
254		
255		
256		
257		
258		
259		
260		
261		
262		
263		
264		
265		
266		
267		
268		
269		
270		
271		
272		
273		
274		
275		
276		
277		
278		
279		
280		
281		
282		
283		
284		
285		
286		
287		
288		
289		
290		
291		
292		
293		
294		
295		
296		
297		
298		
299		
300		
301		
302		
303		
304		
305		
306		
307		
308		
309		
310		
311		
312		
313		
314		
315		
316		
317		
318		
319		
320		
321		
322		
323		
324		
325		
326		
327		
328		
329		
330		
331		
332		
333		
334		
335		
336		
337		
338		
339		
340		
341		
342		
343		
344		
345		
346		
347		
348		
349		
350		
351		
352		
353		
354		
355		
356		
357		
358		
359		
360		
361		
362		
363		
364		
365		
366		
367		
368		
369		
370		
371		
372		
373		
374		
375		
376		
377		
378		
379		
380		
381		
382		
383		
384		
385		
386		
387		
388		
389		
390		
391		
392		
393		
394		
395		
396		
397		
398		
399		
400		
401		
402		
403		
404		
405		
406		
407		
408		
409		
410		
411		
412		
413		
414		
415		
416		
417		
418		
419		
420		
421		
422		
423		
424		
425		
426		
427		
428		
429		
430		
431		
432		
433		
434		
435		
436		
437		
438		
439		
440		
441		
442		
443		
444		
445		
446		
447		
448		
449		
450		
451		
452		
453		
454		
455		
456		
457		
458		
459		
460		
461		
462		
463		
464		
465		
466		
467		
468		
469		
470		
471		
472		
473		
474		
475		
476		
477		
478		
479		
480		
481		
482		
483		
484		
485		
486		
487		
488		
489		
490		
491		
492		
493		
494		
495		
496		
497		
498		
499		
500		
501		
502		
503		
504		
505		
506		
507		
508		
509		
510		
511		
512		
513		
514		
515		
516		
517		
518		
519		
520		
521		
522		
523		
524		
525		
526		
527		
528		
529		
530		
531		
532		
533		
534		
535		
536		
537		
538		
539		
540		
541		
542		
543		
544		
545		
546		
547		
548		
549		
550		
551		
552		
553		
554		
555		
556		
557		
558		
559		
560		
561		
562		
563		
564		
565		
566		
567		
568		
569		
570		
571		
572		
573		
574		
575		
576		
577		
578		
579		
580		
581		
582		
583		
584		
585		
586		
587		
588		
589		
590		
591		
592		
593		
594		
595		
596		
597		
598		
599		
600		
601		
602		
603		
604		
605		
606		
607		
608		
609		
610		
611		
612		
613		
614		
615		
616		
617		
618		
619		
620		
621		
622		
623		
624		
625		
626		
627		
628		
629		
630		
631		
632		
633		
634		
635		
636		
637		
638		
639		
640		
641		
642		
643		
644		
645		
646		
647		
648		
649		
650		
651		
652		
653		
654		
655		
656		
657		
658		
659		
660		
661		
662		
663		
664		
665		
666		
667		
668		
669		
670		
671		
672		
673		
674		
675		
676		
677		
678		
679		
680		
681		
682		
683		
684		
685		
686		
687		
688		
689		
690		
691		
692		
693		
694		
695		
696		
697		
698		
699		
700		
701		
702		
703		
704		
705		
706		
707		
708		
709		
710		
711		
712		
713		
714		
715		
716		
717		
718		
719		
720		
721		
722		
723		
724		
725		
726		
727		
728		
729		
730		
731		
732		
733		
734		
735		
736		
737		
738		
739		
740		
741		
742		
743		
744		
745		
746		
747		
748		
749		
750		
751		
752		
753		
754		
755		
756		

RUSSIAN AND ENGLISH TRIGONOMETRIC FUNCTIONS

Russian	English
sin	sin
cos	cos
tg	tan
ctg	cot
sec	sec
cosec	csc
sh	sinh
ch	cosh
th	tanh
cth	coth
sch	sech
csch	csch
arc sin	\sin^{-1}
arc cos	\cos^{-1}
arc tg	\tan^{-1}
arc ctg	\cot^{-1}
arc sec	\sec^{-1}
arc cosec	\csc^{-1}
arc sh	\sinh^{-1}
arc ch	\cosh^{-1}
arc th	\tanh^{-1}
arc cth	\coth^{-1}
arc sch	\sech^{-1}
arc csch	\csch^{-1}
<hr/>	
rot	curl
lg	log

RADIOSOUNDING OF ICE

V. V. Bogorodskiy

Gidrometeoizdat, Leningrad, 1975

The physical fundamentals of ice sounding based on the pulse radar method are presented in concise form which is accessible for a wide range of readers, and the electromagnetic characteristics of various ices and ~~teh~~ techniques for their measurements are also presented. Also discussed are the fundamentals of pulse radar use for sounding such comparatively strongly absorbing media as sand and permafrost, including permafrost soils and freshwater bodies. The volume is intended for oceanologists, hydrologists, and other specialists involved with problems of ice physics.

FOREWORD

Man is studying the earth on ever increasing scales. The considerable successes achieved in this direction in recent decades have led to the formation of new branches of science -- atmosphere physics, ocean physics, earth physics. At the same time ice, which is found in large quantities in the liquid, solid, and gaseous shells of our planet, has essentially been ignored by the earth physical sciences. Ice is studied in glaciology and cryology -- branches of science which use in considerable measure the geographical and descriptive methods. However, the role of ice, comprising entire systems, is very significant in the geophysical phenomena taking place on the planet. At the present time the attention to and direct interest in ice are constantly increasing in connection with the development of the circumpolar regions, the arctic sea shelf, the Arctic Ocean, and Antarctica. Ice has now become the object of broad study by the specialists not only of those countries which have territories adjacent to the polar regions, but also of many other countries.

The increased interest in ice, both as a physical body and as ice sheets (complex geophysical systems) is easily explained. Ice is a remarkable model of a proton dielectric -- a viscoelastic body which upon comparatively small changes of the external conditions alters its micro- and macro-structure and its electrical and mechanical properties. Ice is both an obstacle for navigation on the seas, oceans, rivers, and a structural material. The continental and mountain glaciers are sources of pure water and are the basic water resources for irrigating the arid lands of Central Asia. The glaciers and ice sheets are in considerable degree regulators of the weather and climate.

We can also mention the influence of ice on life on our planet and practical activity in man. For our country, which as eloquently expressed by Mendeleev, "faces the north," the importance of integrated study of ice is difficult to overestimate. In recent years Soviet and foreign scientists have carried out extensive laboratory and field studies of ice. We can consider that these studies form the basis of ice physics.

We shall examine one of the important technical advances based on the latest achievements in ice physics -- radiosounding of ice. The successful resolution of this complex problem became possible as a consequence of the accumulation of a large amount of data on the electromagnetic characteristics of various ices. At the present time radiosounding of ice based on use of the pulse radar method has been introduced into practice in the study of the antarctic and arctic glaciers and the temperature latitude glaciers. The question of the radiosounding of drifting sea ice has been resolved in principle.

The thickness and rate of movement of the sheet-type glaciers and also their effective temperature and the mass of water concentrated in them can be measured very efficiently by the radar method. It is clear from foreign publications and the information obtained during contacts with scientists of the U.S.A., Canada, the Scandinavian and other countries that this method is being used more and more widely in studying the natural medium. This was confirmed at the First International Symposium on Physical Methods of Studying Ice and Snow, held in Leningrad in October, 1973.

The book presents basically the results of studies by the Arctic and Antarctic Scientific-Research Institute, performed by Trepov, Tripol'nikov, Fedorov, Khokhlov and others. We have also used the materials of certain other Soviet and foreign studies conducted in recent years in the field of radioglaciology.

The author wishes to express his gratitude to G. Ye. Smirnov for valuable suggestions during review of the manuscript and to B.A. Fedorov for his considerable assistance in preparing ~~the~~^{and} discussing the materials included in the book. The author hopes the book will be useful to oceanologists, hydrologists, and other specialists involved with the problems of ice physics.

1. ICE AS AN OBJECT OF GEOPHYSICAL STUDY

Ice, one of the aggregative states of water and the product of metamorphism of snow, is very widely distributed on our planet. The total volume occupied on the earth by glacial ice amounts to about 25 to 30 million cubic kilometers, with nearly 90% of it concentrated in Antarctica. This is a truly astronomical quantity: there is enough ice to cover the entire earth with a layer about 60 meters thick. Colossal masses of ice are also present in the permafrost zone, whose overall area amounts to nearly 20 million square kilometers. The drifting ice cover of the Arctic Ocean contains about 60,000 cubic kilometers of ice.

Approximately 60 million square kilometers of the land surface periodically experiences strong cooling, as a result of which the ground waters lying close to the surface and also the river and lake waters freeze, forming approximately 10,000 cubic kilometers of ice.

Tremendous masses of pure fresh water are concentrated in the glaciers. These supplies exceed by 30 times the mass of all the water resources of the land surface and by more than 40 times the amount of annual precipitation. In the U.S.S.R., glaciers occupy 75,000 KM², about one-third of this area lies under mountain glaciers. More than 10⁴ cubic kilometers of water are present in the glaciers of the U.S.S.R. This mass of water exceeds by several times the annual runoff of all our rivers. The mountain glaciers of the arid regions are very important for agriculture. Their intense melting in the dry seasons and in years when the need for water is particularly acute increases markedly the flow of the rivers which they feed. As glaciers move, they alter the relief significantly, displacing and then depositing tremendous masses of moraine material: clays, sands, and boulders.

The ice mantle of the Arctic is more dynamic than the glaciers. The ice fields drift continuously under the action of the wind and

currents. The nonuniformity and irregularity of the forces acting on these ice fields lead to the occurrence in the ice fields of a complex stress state which may reach the critical stress, after which the thick ice fields begin to crack, break up, and form hummocks. The drifting ice fields, particularly in the periods of their compression, are the primary obstacle to navigation along the Northern Seaway.

Ice -- both as an element and as a physical body -- is full of contradictions. It conceals an entire continent from study and utilization, interrupts or interferes markedly with navigation, cements the soil, destroys coasts, ports, bridges. Man is forced to combat ice. On the other hand, ice is a source of fresh water and a useful constructional material, from which nature creates inexpensive, reliable and comparatively long-lived roads, river crossings, takeoff and landing strips, and floating islands for drifting scientific-research stations. Ice serves mankind broadly.

We note that ice formation and retention of its mass involve the expenditure of a colossal amount of energy. Thus, the transformation of one cubic kilometer of water at temperature $+5^{\circ}\text{C}$ into ice at temperature -10°C under ideal thermostatic conditions requires nearly the same amount of energy provided by all the electric power stations of such developed capitalistic countries as France or Italy in the course of a year. The gigantic energy capacity of the ice formation process poses an important problem of global nature associated with study of the changes of the ice mass on the planet, since this ice mass is both a product of the climate and an indicator of climatic changes on the earth.

2. PHYSICAL METHODS OF ESTIMATING ICE MASS

The practical use of ice in various economic activities, the estimation of the degree of its influence on the geophysical processes and effect on various structures, and the calculation of the amount of water accumulated in the ice lead to the problem of measuring the ice

mass, evaluating its state and rate of movement. In order to calculate the mass we need to know the extent of the ice and its thickness. The determination of the ice layer thickness obviously causes the most difficulty.

Several physical methods have been used in recent years to measure sheet glacier thickness: gravimetric, magnetometric, seismoacoustic, and vertical electrosounding. The seismoacoustic method has found the broadest application. This method was first used by Matthes in 1926 to measure the thickness of alpine glaciers. The studies of Matthes created the basis for seismosounding of glaciers. The seismoacoustic method makes it possible to obtain glacier thickness [24] by direct measurements of the velocity and time of signal propagation in the body of the glacier.

The physical basis of the seismoacoustic method lies in reflection of the sound wave from the interface of two media having different acoustical characteristics. The sound waves, usually excited by an explosion in the medium under study, propagate from the disturbance source in the form of spheres. As they encounter another medium (the glacier bed, for example), the spherical waves reflect from this medium and after some time interval are recorded by the receiver. The time interval t between radiation and reception of the acoustic pulse is proportional to twice the distance traveled by the pulse in the medium under study and its propagation velocity.

In the simplest case of plane-parallel layer thickness measurement the sound pulse source and receiver are separated; the formula for determining the ice layer thickness will have the form:

(1)

where c = explosion pulse propagation speed in the ice; t = time interval (delay) between radiation and reception; D = distance between radiator and receiver. If D is small [1] simplifies and the measured ice thickness will be determined only by the quantities c and t .

Seismoacoustic glacier studies have continued for about 50 years. The seismic method was first used in Antarctica in the fifties. A major role was played by G. K. Robin in this work. In the last 15 to 17 years, since the Norwegian, British, Swedish and French polar expeditions of 1950, the investigators of the U.S.S.R., U.S.A., France, Great Britain, Australia, Belgium, and Japan have conducted major studies to measure glacier thicknesses and determine the nature of the Antarctic continent rock bed relief.

By 1970 seismoacoustic sounding of the glacial mantle had been conducted at more than 1000 points along 50,000 KM-long profiles. A map of the Antarctic glacial mantle thickness was drawn on the basis of the results obtained. The maximal ice thickness (4000 meters) was noted on the two largest Antarctic plains: East and West. The total Antarctic ice volume was established as 24 million cubic kilometers, which is equivalent to 56-meter rise of the world ocean level if the Antarctic ice were to melt. The direct and indirect data obtained made it possible for the first time to draw a schematic map of the Antarctic sub-ice relief. The mountain massifs discovered beneath the glacial shield were termed the Gamburstsev, Vernadskii, Golitsyn, and Shchukin Mountains. Vast plains were also discovered: Schmidt, East, and West. Seismoacoustic sounding made it possible for Soviet and foreign scientists to obtain the first ideas of the bedrock structure of Eastern Antarctica.

More detailed seismoacoustic studies conducted by foreign scientists in Greenland also led to several scientific discoveries. The Greenland glacier bed profile and data on its thickness are appearing in many publications at the present time. Soviet specialists have made extensive seismic studies in accord with the IGY program on glaciers of the Spitzbergen Archipelago, in Central Asia, and other regions.

In addition to solution of very important problems concerning study of glacier bed structure and thickness, the seismoacoustic method has made it possible to gather a large quantity of data on

longitudinal and transverse wave velocity in different glaciers and calculate the important glacier ice physical characteristics: Young's modulus and shear modulus, and the Poisson ratio. However, the primary drawbacks of the seismoacoustic method -- impossibility of remote thickness measurements, low productivity, and very high labor content -- have made it necessary to seek another method which is free of these serious drawbacks.

Pulse Radar Method of Studying the Ice Mantle.

In 1958 the present author and V. N. Rudakov proposed a new method for determining glacier thickness based on the use of pulse radar. The radar (electromagnetic) method, just as the seismoacoustic method, is a direct remote method. It permits measurement of glacier thickness from airplanes, helicopters, tractor-sled trains, and in this regard differs markedly from the seismoacoustic method and utilizes electromagnetic waves radiated as short pulses into the medium under study -- the glacier. The physical essence of this method is as follows: the short electromagnetic pulse radiated by the antenna from some carrier vehicle reaches the glacier surface after a definite time interval and, partly reflecting from this surface, penetrates into the depth of the glacier. The pulse propagates in the body of the glacier and after reaching the bed, reflects from the latter and returns to the receiving antenna. Consequently, the electromagnetic pulse travels a double distance in the glacier -- from the glacier surface to its bed and back. A definite time t is expended in traveling this distance. If we know the velocity c_i of electromagnetic pulse propagation in the glacier the thickness can be found from the formula:

$$h = \frac{c_i t}{2}; \quad (2)$$

The time delay t is determined from the radar indicator scale. We note that the thickness measurement error does not exceed 2 - 2.5% and the time of continuous thickness measurement along unit length of the path being studied is determined by the carrier vehicle speed. Thus the electromagnetic signal delay time and signal velocity in the

body of the glacier make it possible to determine glacier thickness rapidly and with high accuracy [5].

At the present time, the radar method is wisely used in practice and has become the basic working "tool" of Soviet and foreign research glaciologists for measuring the thickness of the glaciers of Antarctica, Greenland, and other regions. It is also being used with success in studying temperature and mountain glaciers [6, 8].

The pulse radar method, very effective in remote measurement of the thickness of various glaciers, is now also widely used to study their structure and state (introscopy). For example, this method makes it possible to measure the average (effective) glacier temperature, determine the density nonhomogeneity and other nonhomogeneities through its thickness, measure glacier velocity, and identify crevasses hidden by snow bridges. The radar method is now being used to measure the thickness of drifting sea ice and study its properties. Finally, radar glacier studies have made it possible to advance well-founded suggestions on the possibility of using the pulse radar method for studying media with dielectric losses higher than those of ice: sands, permafrost, and freshwater bodies. We see that this method makes it possible to solve successfully a large range of problems. There is basis to believe that the pulse radar method will in the near future be introduced successfully into many geophysical studies.

Ice radiosounding is now based on extensive theoretical and experimental studies; they are discussed in the following sections.

3. STRUCTURE AND ELECTROMAGNETIC PROPERTIES OF GLACIERS. ELECTROMAGNETIC WAVE PROPAGATION IN GLACIERS.

Glacier Structure.

In accord with the Avsyuk classification [1] the largest glaciers on earth -- the glaciers of Antarctica -- are dry polar glaciers.

The temperature of their mass is always below 0°C, and consequently melting of the ice in the body of the glaciers does not take place. Temperature changes take place only in the surface layer of thickness about 12 meters, and decay below this level (Figure 1).

Glaciers have marked stratified structure. The surface layer is snow. At negative temperatures the snow layer, primarily as a result of recrystallization, transforms into so-called recrystallization firn. The density of cold recrystallization firn is 0.5 g/cm³ or higher [25]. The firn crystals have isometric structure and their average linear dimensions do not exceed 1 - 1.5 cm.

The firn also lies as a layer. The thickness of the firn layer varies, for example for Antarctic glaciers in the coastal zone, the thickness is about 20 meters. In the cold firn band the firn reaches thicknesses of 40 meters and more. Thus, according to the data of the Third Soviet Antarctic Expedition (SAE) the firn layer thickness in the Pioner Station region is 120 meters, at the Komsomol'skaya Station the thickness is 137 meters, and at the South Pole the thickness is 164 meters. The firn layer in turn (for example, according to the data of Kotlyakov) has a stratified structure -- more dense layers alternate with less dense layers.

The formation of cold recrystallization ice -- the basic substance of the Antarctic glaciers -- is determined by the moment of disappearance of air permeability of the firn. It has been established experimentally that the firn density at the instance of air permeability disappearance approaches 0.83 g/cm³. The glacier ice layers are the primary and thickest glacier layers. Glacier ice contains certain impurities and inclusions: air bubbles, moraine, cosmic dust, and so on. Their influence on the electromagnetic characteristics of the ice is negligibly small in most cases.

Electromagnetic Properties of Ice.

Ice, one of the basic glacier components, is a crystalline body.

The crystals of conventional ice belong to the hexagonal group.

The hexagonal ring layer plane is termed the crystal basis plane. The direction of the perpendiculars to the basis plane is the optical axis or C axis.

Ice, like water, is a polar (or dipole) dielectric, i.e., a dielectric in the molecules of which the unlike charge centers do not coincide but are located at some distance from one another.

In static fields the electric properties of the dielectrics are usually described by

the static dielectric permeability ϵ_c [3, 22]. In alternating fields the polarization of the dielectric is connected with the field frequency and also with the temperature of the dielectric. In the radio-frequency band ice has anomalous dispersion, dielectric permeability, and absorption. This phenomenon was explained by Debye, who assumed that the individual molecules rotate under the action of the applied field. On the basis of his theory, Debye obtained analytic expressions, with the aid of which the dielectric properties of ice are well described in a wide range of frequencies, and specifically in the ratio frequency band:

$$\epsilon' = \frac{\epsilon_c + \epsilon_\infty (\omega\tau)^2}{1 + (\omega\tau)^2}, \quad (3)$$

$$\operatorname{tg} \delta = \frac{\epsilon''}{\epsilon'} = \frac{(\epsilon_c - \epsilon_\infty) \omega\tau}{\epsilon_c + \epsilon_\infty (\omega\tau)^2}, \quad (4)$$

where ϵ' and ϵ'' are the real and imaginary parts of the complex relative to dielectric permeability ϵ ($\epsilon = \epsilon' - j\epsilon''$); $\operatorname{tg} \delta$ — the tangent of

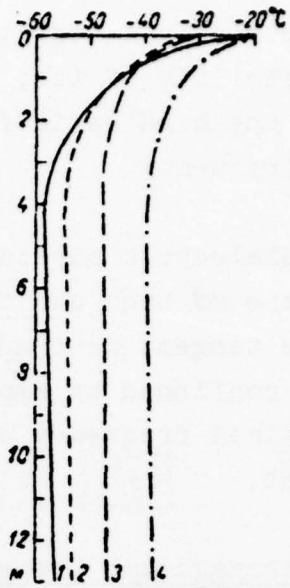


Figure 1. Temperature distribution in upper part of snow-firn layer in Antarctic glacier in the summer. 1- Vostok Station; 2- Komsomol'skaya Station; 3- Vostok-1 Station; 4- Pioner Station.

the dielectric loss angle; $\epsilon_c = 93$ (for -10°C) is the static dielectric permeability of ice; $\epsilon_\infty = 3.17$ is the dielectric permeability of ice in the high radio-frequency band; τ = relaxation time; ω = circular frequency.

The dielectric permeability maintains an approximately constant value in the rf band and at low temperatures, while the dielectric loss angle tangent decreases with frequency. Both of these relations have been confirmed by experiments, which makes it possible to select optimal frequency bands and temperatures for radar system development.

BEST AVAILABLE COPY

Electromagnetic Properties of Snow and Firn in the RF Band.

Snow and firn should be considered a heterogeneous two-component system consisting of a statistical mixture of dielectrics -- pure ice and air. At negative temperatures the dielectric parameters of snow and firn can be defined as the characteristics of a complex dielectric consisting of two components: pure ice and air. For their determination we can use the Lichtenecher equations [4]:

$$\dot{\epsilon}_r = Q_1 \dot{\epsilon}_{r,1} + Q_2 \dot{\epsilon}_{r,031}, \quad (5)$$

where $\dot{\epsilon}_{r,1}$, $\dot{\epsilon}_{r,031}$, $\dot{\epsilon}_{r,031}$ are, respectively, the complex relative dielectric permeabilities of real ice, pure ice, and air; Q_1 and Q_2 are the volumetric concentrations of the components, where $Q_1 + Q_2 = 1$; x = constant quantity for given distribution of the components.

Particular cases are as follows:

1. If the dielectrics (pure ice and air) are arranged parallel to the vector E , then $x = 1$ and (5) takes the form:

$$\dot{\epsilon}_r = Q_1 \dot{\epsilon}_{r,1} + Q_2 \dot{\epsilon}_{r,031}. \quad (6)$$

This expression must be used, for example, when there are horizon-

tally oriented air cavities in the ice and the electromagnetic wave, polarized horizontally, propagates horizontally, or the vertically polarized wave propagates vertically.

2. If the electrics are arranged sequentially relative to the vector E , then $x = -1$ and (5) takes the form:

$$\frac{1}{\epsilon_1} = Q_1 \frac{1}{\epsilon_{4,1}} + Q_2 \frac{1}{\epsilon_{8031}}. \quad (7)$$

This will correspond to horizontal propagation of the vertically polarized wave in a glacier with horizontally aligned air interlayers.

3. Finally, the most typical case, when pure ice and air are "mixed" chaotically and the linear dimensions of the ice and air formations are considerably less than the length of the electromagnetic wave. In the case of chaotic distribution the component $x = 0$. Expanding the terms of (5) into power-law series, we obtain:

$$\ln \epsilon_1 = Q_1 \ln \epsilon_{4,1} + Q_2 \ln \epsilon_{8031}. \quad (8)$$

BEST AVAILABLE COPY

For air in a wide range of frequencies and pressures the dielectric parameters are identical to those for vacuum ($\epsilon'_{8031} = 1$, $\epsilon''_{8031} = 0$). Since for ice at frequencies above 10^7 Hz $\lg \delta \ll 1$, Equations (5) - (8) can be used directly for calculating ϵ' , substituting therein $\epsilon'_{4,1}$ and ϵ'_{8031} . The dependence of ϵ' on glacier material, calculated using (8), is shown for the 213 MHz frequency in Figure 2. In the calculations we used the following basic data: ice density $\rho = 0.915 \text{ g/cm}^3$, ice relative dielectric permeability $\epsilon'_{4,1} = 3.35$. (after Hippel).

Electromagnetic Wave Propagation in Glaciers.

We noted above that the relative dielectric permeability of ice is complex:

$$\epsilon = \epsilon' - j\epsilon'' = \epsilon' (1 - j \lg \delta). \quad (9)$$

The relative magnetic permeability of ice is taken as one. Considering this situation and using the Maxwell equation, we can obtain the fundamental solution of the problem of monochromatic wave propagation in a glacier [18].

The solution for the vector E of the wave equation with complex wavenumber $k(z) = \frac{\omega}{c} \sqrt{\epsilon_s(z)}$,

which is a function of the z coordinate, is written in the form:

$$E = \frac{A}{\sqrt{k(z)}} e^{-i \int k(z) dz} \quad (10)$$

where $A = \text{constant}$.

We consider that the electromagnetic properties of the glacier vary along the vertical (z axis) because of the variation of its density and temperature and write the complex wavenumber in explicit form:

$$k(z) = \alpha(z) - i\beta(z); \quad (11)$$

Here $\alpha(z)$ = propagation coefficient:

$$\alpha(z) = \frac{\omega}{c} n(z) = \frac{\omega}{c} \sqrt{\frac{\epsilon_s}{2} (V 1 + \lg^2 i + 1)}; \quad (11a)$$

$n(z)$ = refraction index; $\beta(z)$ = attenuation coefficient:

$$\beta(z) = \frac{\omega}{c} k(z) = \frac{\omega}{c} \sqrt{\frac{\epsilon_s}{2} (V 1 + \lg^2 i - 1)}; \quad (11b)$$

$k(z)$ = attenuation index.

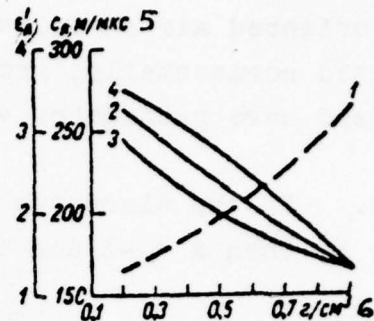


Figure 2. ϵ_r and μ_r as functions of density of glacier material for 213 MHz frequency. 1- ϵ_r for chaotic distribution of components --pure ice and air; 2- ϵ_r for chaotic distribution of components; 3- ϵ_r for parallel arrangement of components; 4- ϵ_r for series arrangement; 5- μ_r ; 6- $m/\mu s$.

The time interval t required for double electromagnetic wave travel through a glacier of thickness h (before and after reflection from the bed) is determined from the expression:

(12)

$$t = \frac{2}{c} \int a(z) dz = \frac{2}{c} \int n(z) dz.$$

If the refraction index varies little along the vertical ($n = \text{const}$), then

$$t = \frac{2nh}{c} = \frac{2h}{c_s}. \quad (13)$$

where c_s = electromagnetic wave velocity in the glacier; c = electrodynamic constant.

In the real glacier the refraction index increases with depth, due primarily to the density increase, therefore it is necessary to consider the variation of n as a function of the coordinate z . For known distribution of the density ρ across the section of the glacier the integral in (12) can be found approximately. The glacier thickness is broken down into m uniform layers with refraction index n_k and thickness h_k :

$$\bar{n}h = \sum n_k h_k \quad (14)$$

where \bar{n} = "effective" refraction index for the glacier with known density distribution through the thickness.

It follows from (13) and (14) that the time interval t is determined by the refraction index \bar{n} and thickness of the glacier. The effective electromagnetic wave velocity in the glacier:

$$c_s = \frac{c}{\bar{n}} \quad (15)$$

Taking for the frequency $f = 213$ MHz $\bar{n} = 3.35$ (after Hippel), we find from (15) that $c_s = 169$ m/ μ sec.

Analysis made on the basis of (6) and (7) showed that for ice of density 0.917 g/cm^3 (see Figure 2) the electromagnetic wave velocity does not depend on the positioning of the dielectrics in relation to the direction of the vector E , but for lower densities there is some such dependence. The calculation of the velocity \bar{c}_n as a function of the coordinate z (and consequently of ρ) for Greenland ice is shown in Figure 3. It is clear that the smaller the thickness of the snow-firn layer in relation to the overall thickness of the glacier, the closer the quantity \bar{c}_n approaches the electromagnetic wave velocity in pure ice.

The results of specific calculations are as follows. For pure ice $\epsilon'_{n,n} = 3.35$ and $\bar{c}_n = 164 \text{ m}/\mu\text{sec}$. The thickness of the snow-firn layer (with density $0.82 - 0.84 \text{ g/cm}^3$) for the Greenland borehole is 73 meters. For the depth $z = 200 \text{ meters}$ $\bar{c}_n = 175 \text{ m}/\mu\text{sec}$, for $z = 300 \text{ meters}$ $\bar{c}_n = 171 \text{ m}/\mu\text{sec}$, and for $z = 400 \text{ meters}$ $\bar{c}_n = 169 \text{ m}/\mu\text{sec}$.

It follows from (10) with account for the complex nature of the wavenumber that as the electromagnetic signal propagates in the glacier its intensity decreases because of absorption. The degree of signal attenuation (in dB) can be found from the formula:

$$N_n = 20 \lg \frac{E_0}{E} \quad (16)$$

where E_0 = radiated signal intensity; E = received signal intensity.

For plane waves which have twice traversed a glacier of thickness h we obtain:

$$N_n = 17.36 \int \beta(z) dz = 17.36 \frac{h}{c} \int k(z) dz \quad (17)$$

For high frequencies $\lg \delta \ll 1$. Assuming constancy of $\operatorname{tg} \delta$ through the thickness of the glacier, we obtain the final expression for N_n :

$$N_n = 8.68 \frac{h}{c} \sqrt{\epsilon_n h \operatorname{tg} \delta} \quad (18)$$

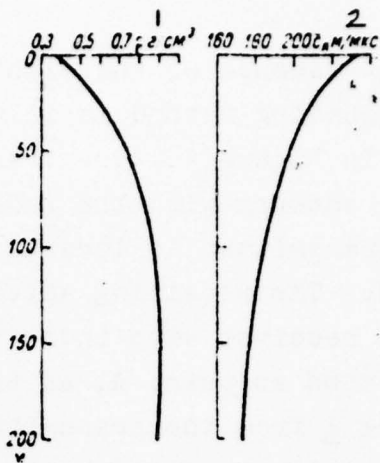
Thus, from theoretical examination of electromagnetic wave propagation in a glacier we have obtained on the basis of solution of the wave equation (10) the time lag between the radiated (sounding) and received radar signals and the magnitude of the absorption. These quantities make possible quite accurate determination of the parameters of radars for glacier thickness measurement. Electromagnetic wave propagation in glaciers is also accompanied by other losses. They will be examined later.

4. EXPERIMENTS TO DETERMINE ELECTROMAGNETIC CHARACTERISTICS OF GLACIERS

Measurements of Electromagnetic Wave Propagation Velocity.

It follows from (13) that knowledge of the electromagnetic wave velocity for the problem under consideration is very important, since it determines the accuracy of the method. The most reliable method for measuring electromagnetic wave velocity is the slant sounding method. This method was used successfully by Gudmandsen in Greenland and by Trepov and Jiracek in Antarctica.

The constancy of the electromagnetic wave propagation velocity in ice in a broad frequency range (from 10 to 2700 MHz), its small variation as a function of temperatures existing in natural glaciers, and the large amount of data on the structure of these glaciers make it possible to obtain reliable data on the value of c_s for various geographic coordinates and experimental locations.



BEST AVAILABLE COPY

The essence of the slant radio sounding method is illustrated in Figure 4. The transmitting antenna with the radio pulse transmitter is located at point B. The receiving antenna and the receiver with indicator are located at point A, at the distance l from the transmitter. To each pulse radiated by the transmitter correspond two pulses in the receiver: one travels the distance l through the air, the other is reflected from the glacier bed and travels the distance s through the ice (in the figure, point A' is the mirror image of point A relative to the glacier bed). Measuring on the indicator the delay of the second signal relative to the first for different l , we can from geometric relations obtain the velocity of the radio pulse in the ice under the condition that the glacier is homogeneous:

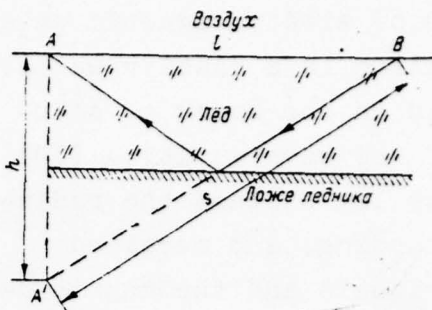


Figure 4. Scheme for determining electromagnetic wave velocity by slant sounding. 1- air; 2- ice; 3- glacier bed.

BEST AVAILABLE COPY

$$\frac{t_s^2 c^2}{\epsilon_1} = (2h)^2 + l^2, \quad (19)$$

where t_s = radio wave propagation time from the transmitting antenna to the receiving antenna through the ice layer.

From (19) follows:

$$t_s^2 = \frac{\epsilon_1}{c^2} l^2 + \frac{\epsilon_1}{c^2} (2h)^2, \quad (20)$$

i.e., the square of the radio pulse propagation time from the transmitting antenna to the receiving antenna depends linearly on the square of the distance l , and the slope of the line $\frac{\epsilon_1}{c^2}$ is the inverse of the square of the electromagnetic wave propagation velocity in the ice.

Consequently, the determination of radio wave propagation velo-

ity in the ice reduces to obtaining the experimental relation $t_s^2 = \tau(l^2)$, approximating the experimental relation by a straight line, and determining the slope of this approximating line. The time t_s is found as the sum of the delay time t_3 of the pulse traveling through the ice relative to the pulse propagating in the air (measured on the indicator) and the time $t_1 = \frac{l}{c}$ of pulse propagation through the air. The distance l is measured.

The experiments were conducted as follows. The mobile receiving and transmitting sets were moved in opposite directions along a pre-determined rectilinear survey line so that the reflecting bed segment remained the same in the process of the measurements. Measurements were made every 50 meters of the lag of the pulse reflected from the bed relative to the pulse traveling through the air. Preliminary measurements of the glacier thickness were made before starting the study in order to select a segment with constant thickness. The results of velocity measurements using a radar with carrier frequency 440 MHz, obtained by the 14th SAE [20] along one survey line near the Molodezh Station are shown in Table 1.

TABLE 1

l m	0	50	100	150	200	250	300	350
t_3 MKC	2.25	2.0	1.85	1.72	1.7	1.7	1.75	1.83
t_1 MKC	0	0.165	0.33	0.5	0.66	0.83	1.0	1.165
t_s MKC	2.25	2.165	2.18	2.22	2.37	2.53	2.75	2.995
$l^2 \cdot 10^{-4}$ m ²	0	0.025	1	2.26	4	6.25	9	12.27
t_s^2 MKC ²	5.08	4.7	4.75	4.93	5.41	6.4	7.57	8.95

1- μ s; 2- μ s²

BEST AVAILABLE COPY

It is well known [16] that the slope of the straight line approximating the experimental linear relation $y = a + bx$ between two random quantities x and y when using the least squares method is defined by

the expression

$$b = r \sqrt{\frac{(y - \bar{y})^2}{(x - \bar{x})^2}} \quad (21)$$

where r = coefficient of correlation between x and y .

The results of measurements of $R = \rho(R)$ along seven survey lines are shown in Figure 5. The measured radio wave velocities 167.8, 168.6, 170 and 178 m/ μ sec, obtained near the Antarctic shoreline, and 184.5 m/ μ sec obtained 45 km from the coast, agree well with the data calculated using the average glacier density. The experimental data basically confirm the validity of the velocity $\bar{c}_n = 169$ m/ μ sec used for the calculations. Analysis of the measurement error showed that the basic error apparently occurs in reading out the time interval between the pulses, since for a baseline length approximately equal to the glacier thickness this interval is short (in our case, 0.55 μ sec) and is comparable with its readout accuracy. In order to reduce this error we must make measurements on a baseline with $l \geq 2 - 3h$. Such measurements are possible with small glacier thicknesses.

In the case of long baselines, when the wave incidence angles on the glacier surface are large, error may arise due to refraction at the air-glacier interface and in the upper layers of the glacier, which have variable coefficients of refraction. In this case as a result of increase of the path length in the layer with smaller refraction coefficient the radio wave velocity will be higher than the velocity obtained at smaller incidence angles. However, this error is systematic and can be taken into account theoretically on the basis of data on the antenna height above the glacier surface and the density vertical distribution.

Table 2 shows the velocities obtained by the 15th SAE. The measurements were made at a 440 MHz frequency at three points in the Molodezh Station region. At each point the measurements were made on three different survey lines with the use of parallel and orthogonal

receiving dipoles.

In the 16th SAE velocity measurements were made for the first time at 60 MHz frequency. The use of a powerful radar set made it possible to conduct measurements in regions with large glacier thickness. Measurements were made at six points on a survey line to the south of Molodezh Station. The measurement results are shown in Table 3.

Jiracek (USA), using a similar method, obtained at the 30 MHz frequency the following radio wave propagation

velocities in ice: with glacier thickness from 170 to 320 meters $c_s = 180 \pm 5$ m/ μ sec, on the 760 m-thick Skelton Glacier (without snow-firn cover), $c_s = 168.5$ m/ μ sec, on the Roosevelt Glacier with thicknesses 500 and 800 meters $c_s = 174.8$ m/ μ sec. These velocities make it possible to obtain the average dielectric permeability and refraction index of radio waves for the glaciers located in the region of the experiment.

TABLE 2

Measurement line identification No.	1	2	3	1	2	3	1	2	3
Average glacier thickness along line, m	300	300	309	426	568	465	367	384	375
Radio wave velocity in ice, m/ μ sec.	163	170	156	185	170	183	179	172	176

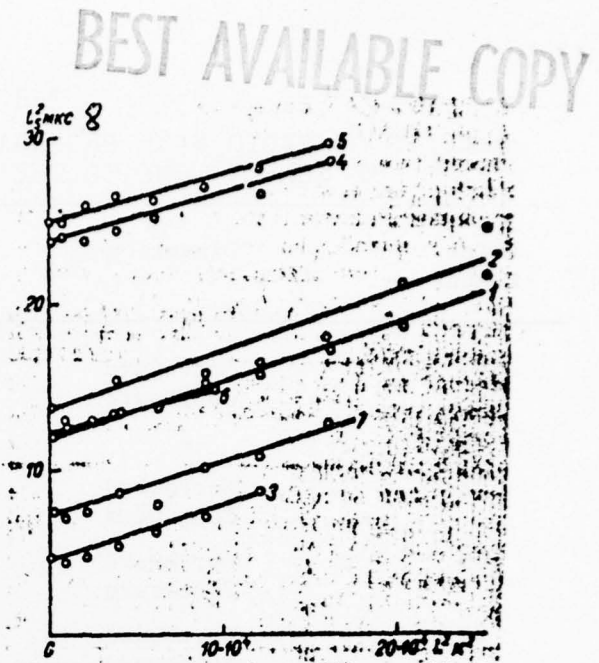


Figure 5. Experimental data and approximating curves of t_s^2 versus 1^2 . Average values of c_s : 1- 168.6 m/ μ sec; 3- 178.0 m/ μ sec; 4 & 5- 184.5 m/ μ sec; 6- 172.0 m/ μ sec; 7- 167.0 m/ μ sec; 8- μ s.

TABLE 3
RESULTS OF RADIO WAVE PROPAGATION VELOCITY MEASUREMENT IN ICE
ON SURVEY LINE TO THE SOUTH OF MOLODEZH STATION

Point Number	Direction	Radio Wave Velocity, m/μs	Glacier Thickness, m
43	Northward	172	820
	Southward	160.5	
46	--	167.0	597
22	Northward	182.0	860
	Southward	172.5	
109	Northward	162.5	650
	Southward	169	
26	Northward	153	1330
	Southward	154	
73	Northward	160	313
	Southward	170	

Study of Dielectric Losses in Antarctic Glaciers.

It was mentioned above that ice is a dielectric having complex dielectric permeability. The imaginary part of the complex dielectric permeability determines the magnitude of the dielectric losses. To characterize the ability of a dielectric to absorb electromagnetic field energy, we generally use the dielectric loss angle tangent $\operatorname{tg} \delta$, which is defined as the ratio of the two components of the complex dielectric permeability or as the ratio of the active conductivity of the imperfect dielectric to its capacitive conductivity, i.e.,

$$\operatorname{tg} \delta = \frac{\epsilon''}{\epsilon'} = \frac{\gamma_a}{\omega \epsilon_0}.$$

The tangent of δ is a very important

electromagnetic characteristic and is necessary for calculating electromagnetic wave absorption in ice and selecting the radar potential. Field measurements of $\operatorname{tg} \delta$ are most interesting for the subject problem.

In 1966 the range of $\operatorname{tg} \delta$ values for actual Antarctic ice was calculated indirectly [10]. The data of radar sounding along the route from Mirnyi Observatory to Pioneer Station were used for this

BEST AVAILABLE COPY

TABLE 4

TANGENT OF DIELECTRIC LOSS ANGLE OF REAL ICE (AFTER JIRACEK).

Study Region	Ice Density, g/cm ³	Ice Temperature, °C	tgδ for frequency, MHz		
			150	300	213
Iceland (glacier ice)	0.818	-1	0.0022	0.00108	0.00052
		-5	0.00144	0.00076	0.00040
		-10	0.00110	0.00055	0.00028
		-20	0.00068	0.00033	0.00019
		-30	0.00043	0.00031	0.00013
		-40	0.00026	0.00018	0.00008
		-50	0.00014	0.00008	0.00003
Little America, Antarctica	0.881	-1	0.0037	0.0018	0.00105
		-5	0.0026	0.0013	0.00072
		-10	0.00217	0.00109	0.00058
		-20	0.00154	0.00078	0.00038
		-30	0.00116	0.00057	0.00029
		-40	0.00085	0.00044	0.00023

purpose. After reducing the measurement data a calculation was made of the dielectric losses resulting from absorption for various values of $\text{tg } \delta$, and then the overall losses were evaluated for each assumed value of $\text{tg } \delta$. It was concluded in comparing the experimental and calculated losses that the most reliable average values of $\text{tg } \delta$ at the 213 MHz frequency for the entire thickness of the glacier, including the snow layer, lie in the range $4.2 \cdot 10^{-4} - 7 \cdot 10^{-4}$.

Jiracek presented the most complete data on the values of $\text{tg } \delta$ for real ice in 1967. (Table 4). We see from the table that $\text{tg } \delta$ depends strongly on ice temperature and field frequency.

5. ATTENUATION OF RADIO WAVES IN GLACIERS

Overall Attenuation of Radio Waves During Their Propagation in Glaciers.

It was shown above that radio pulses decay as a result of absorption during passage through a layer of ice. It follows from (18) that radio wave absorption is determined by the radiated frequency (the working frequency f is connected with the circular frequency ω by the relation 1), ice layer thickness, and the quantities ϵ' and $\operatorname{tg} \delta$. Absorption is an irreversible loss of radio wave energy; the field energy is transformed into heat as a result of interaction with the medium.

Radio waves also decay as a result of spreading of their front during propagation in the medium (geometric losses) and reflection on the interfaces (surface, interior density nonhomogeneities, glacier bed). They also change their intensity as a result of the focusing action of the ice layer and noncoincidence of the reflected signal polarization with the receiving antenna polarization. Study of the components of radar signal attenuation during propagation in the various earth covers is important primarily from the viewpoint of optimizing the parameters of radars intended for sounding, and also in refining the electrodynamic models of these covers and studying their electrophysical characteristics.

Radio wave propagation theory and the large amount of experimental data obtained in radar sounding of the Antarctic and Arctic glaciers make it possible to evaluate quantitatively the overall attenuation on the basis of the previously indicated additive components of electromagnetic wave attenuation in ice. The amplitudes of the signals received by the station after their passage through the ice layer are determined by the overall attenuation, which can be expressed by the relation:

$$N_r = N_r + N_{\text{opt}} + N_{\phi} + N_p + N_n + N_{\text{no}}, \quad (22)$$

where N_r = geometric losses; N_{ref} = losses owing to reflecting from the interfaces; N_f = signal change as a result of focusing; N_s = losses as a result of scattering; N_a = losses resulting from absorption; N_{pol} = losses resulting from noncoincidence of the polarization of the signal received by the antenna with the receiving antenna polarization.

We shall consider that the signal reflected by the glacier differs from the radiated signal only in amplitude, time interval, and phase shift. This signal acts together with noise on the receiver input. The noise level is determined by the noise level of the receiving channel, the atmosphere, and the medium being sounded.

If we examine the problem of measuring glacier thickness we can consider that part of the input is the useful signal (in our case the pulses reflected by the glacier bed), while the remainder, consisting of noise and the pulses reflected by the upper boundary and the internal nonhomogeneities of the glacier, is interference. We will not examine the theory of received signal detection and processing; this theory is examined in detail in many specialized monographs and texts. A more important problem is the analysis and evaluation of the terms determining the magnitude of the overall radio signal attenuation during sounding of media.

Absorption

It was shown previously that the dielectric loss angle tangent depends strongly on the temperature of the medium in question. If the vertical temperature distribution through the glacier is known the absorption can be calculated using (17), which takes into account signal propagation toward the glacier bed and back. If $k(z)$ is represented by a complex function of z the losses due to absorption can be evaluated approximately by considering the glacier to consist of a large number of layers with dielectric loss angle tangent which is constant in the limits of each layer. The losses in the layer are calculated from an expression similar to (18):

$$N_n(z) = 8.68 \frac{a}{c} \sqrt{e} \operatorname{tg} \delta dz,$$

(23)

where dz denotes a very small thickness of the layer with constant $\operatorname{tg} \delta$; $N_n(z)$ is the absorption in the layer.

Now we must sum the losses in the layers through the entire thickness of the glacier

$$N_n = \int^h N_n(z) dz, \quad (24)$$

or, if the number of layers is finite (for example m layers)

$$N_n = \sum_1^m N_n(z) \Delta z, \quad (25)$$

where Δz = thickness of layer with practically constant $\operatorname{tg} \delta$. It is obvious that the thinner the layers, the more accurately the approximate expression (25) evaluates the losses, and the closer it approaches the more exact expression (24).

However, in most cases the temperature distribution through the section of the glacier is not known. Therefore it is convenient to characterize the absorbing properties of the glacier body by the so-called absorption temperature t_n , satisfying the expression:

$$N_n = \bar{N}_n(t_n) h, \quad (26)$$

where $\bar{N}_n(t_n)$ is the specific absorption, uniquely defined by the absorption temperature.

The absorption temperature thus characterizes the glacier as a whole, specifically its ability to absorb electromagnetic signals, and is a very important additional thermal characteristic of the glacier, since it makes it possible to differentiate warmer and cooler glaciers without reference to the thickness.

The values of $\bar{N}_n(t_n)$ were calculated on the basis of (18) for unit glacier thickness (per meter) and are shown in Table 5 for the

10 - 500 MHz frequency range.

TABLE 5

BEST AVAILABLE COPY

t_u °C	-1	-5	-10	-20
N_u dB/m	0.1062	0.0709	0.050	0.0322
t_u °C	-30	-40	-50	-60
N_u dB/m	0.0200	0.0129	0.0077	0.0025

1- dB/m

These data make it possible to calculate easily the radio wave energy losses by absorption for any ice temperature.

Geometric Losses and Losses at the Lower Boundary.

In accordance with the radar range expression, we can write for the geometric losses N_r and the reflection losses N_r at the lower boundary for the cases of mirror reflection and scattering with the radar set operating in the near zone*: $\left(h < 20 + 30 \frac{c\tau_{\text{max}}}{2} \right)$

$$N_r + N_{\text{opt}} = -20 \lg G\lambda + 20 \lg h + 10 \lg 64\pi^2 - 20 \lg K_f$$

where $G\lambda$ is determined by the station parameters; G = radar antenna gain; K_f = Fresnel reflection coefficient; for media with small losses and normal incidence:

$$K_f = \frac{\sqrt{\epsilon_1} - \sqrt{\epsilon_2}}{\sqrt{\epsilon_1} + \sqrt{\epsilon_2}}$$

$N_{\text{opt}} = -20 \lg K_f$ and depends on the dielectric permeability of the underlying surface. For the calculation we took $N_{\text{opt}} = 14$ dB.

* Here τ_{max} = duration of rf pulse radiated by the radar.

Summing the geometric losses and the reflection losses, we obtain (in dB):

$$N_r + N_{\text{ref}} = -20 \lg G\lambda + 20 \lg h + 42. \quad (27)$$

Focusing.

Jumping ahead, we shall show that signal attenuation as a consequence of focusing when working from the glacier surface $N_f = -20 \lg n$, where n = coefficient of refraction at the air-ice boundary. When working from an airplane it is necessary to consider the dependence of focusing on the flight altitude.

We shall examine briefly some theoretical aspects of electromagnetic wave focusing when sounding glaciers.

It is well known that in a homogeneous medium at the distance r from a point radiation source the power flux density:

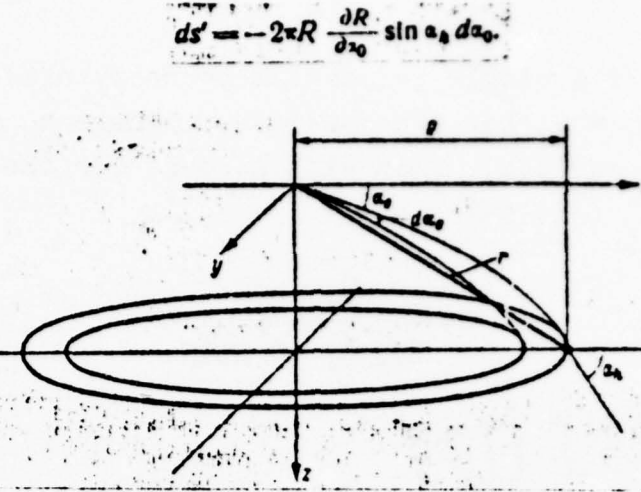
$$I_{\text{f}} = \frac{P_{\text{rad}}}{4\pi r^2}. \quad (28)$$

In a stratified nonhomogeneous medium the power flux density at the same distance will be different because of refraction and equal to I_f . We term the ratio:

$$\eta = \frac{I_f}{I_{\text{f}}}. \quad (29)$$

the focusing factor. We shall determine the focusing factor for a stratified nonhomogeneous medium in which the refraction coefficient n is a function of the z coordinate. The case of two media with a flat interface will obviously be a particular case. In Figure 6 the radiation source is located at the coordinate origin, α_0 = ray glance angle at the exit point; α_h = ray glance angle at the observation point at the depth h . We obtain $ds' = 2\pi R \sin \alpha_h dR$ for the wave front area included between the rays leaving at the angles α_0 and $\alpha_0 + d\alpha$. Considering that $dR = -\frac{\partial R}{\partial \alpha_0} d\alpha$ (the minus sign means that for $h =$

const smaller R correspond to larger α_0), we obtain:



BEST AVAILABLE COPY

Figure 6. Illustration for determining focusing factor for stratified nonhomogeneous medium.

Since the power in the solid angle Ω in the limits from α_0 to $\alpha_0 + d\alpha_0$ is equal to $P_\Omega = \frac{P_{\text{max}}}{2} \cos \alpha_0 d\alpha_0$, the power flux density

at the distance r from the source is:

$$\eta = \frac{P_{\text{max}}}{2} \frac{r \cos \alpha_0}{2\pi R \frac{\partial R}{\partial \alpha_0} \sin \alpha_0} \quad (30)$$

Substituting (28) and (30) into (29), we obtain:

$$\eta = \frac{r^2 \cos \alpha_0}{R \frac{\partial R}{\partial \alpha_0} \sin \alpha_0} \quad (31)$$

In order to calculate the focusing factor using (31) it is necessary to determine R and $R \frac{\partial R}{\partial \alpha_0}$. The final expression for η

has the form:

$$\eta = \frac{\cos^2 \alpha_0 \int_0^h \frac{dz}{[n^2(z) - \cos^2 \alpha_0]^{1/2}}}{\sin \alpha_h \sin \alpha_0 \int_0^h \frac{n^2(z) dz}{[n^2(z) - \cos^2 \alpha_0]^{1/2}}} \quad (32)$$

In the case of a single refracting boundary $n(z) = n_0$ for $0 < z < h_0$ and $n(z) = n_1$ for $h_0 < z < h_0 + h$, where h_0 = antenna height above the glacier surface. Then with account for the relation $\sin \alpha_h = \frac{1}{n} (n^2 - \cos^2 \alpha_h)^{1/2}$ (32) takes the form:

(33)

$$\eta = \frac{\frac{h_0}{\operatorname{tg} \alpha_0} + \frac{h}{\operatorname{tg} \alpha_1}}{\frac{h_0 \sin \alpha_1}{n_0 \sin^2 \alpha_0} + \frac{h \sin \alpha_0}{n_1 \sin^2 \alpha_1}}.$$

BEST AVAILABLE COPY

Table 6 shows the results of calculation of the focusing factor η for radiation passage from a medium with refractive index $n_1 = 1$ (air) into a medium with refractive index $n_1 = 1.5$ (snow with density 0.5 g/cm^3) and back for various glance angles in the first medium (air).

TABLE 6

Glance angle in first medium, degree	1	2	5	10
for $n_0 = 1$ and $n_1 = 1.5$	0.026	0.052	0.13	0.33
for $n_0 = 1.5$ and $n_1 = 1$	0.011	0.023	0.055	0.13
Attenuation for radiation propagation in both directions, dB	35.3	29.3	21.3	15.3

Let us evaluate focusing of electromagnetic energy at small incidence angles (vertical radiosounding). For this case (31) for incidence angles $\beta = 90^\circ - \alpha$ has the form:

(34)

$$\tau_1 = \frac{r^2 \sin \beta_0}{R \frac{\partial R}{\partial \beta_0} \cos \beta_0}.$$

Omitting the intermediate arguments, but considering the rela-

tions, valid for small incidence angles,

$$r = h_0 + h; \cos \beta_0 \approx \cos \beta_1 \approx 1.$$

$$\left. \begin{aligned} \operatorname{tg} \beta_0 &\approx \sin \beta_0 \approx \beta_0 \\ \operatorname{tg} \beta_0 &\approx \operatorname{tg} \beta_1 \approx \beta_1 \end{aligned} \right\} \frac{\beta_0}{h} = \frac{n_1}{n_0}.$$

we obtain the formula for η in the plane interface case:

$$\eta = \frac{\left(1 + \frac{h}{h_0}\right)^2}{\left(1 + \frac{n_0}{n_1} \cdot \frac{h}{h_0}\right)^2}. \quad (35)$$

The focusing factor η' for sounding of the medium is equal to the product of the focusing factors for wave propagation "to" (η_{max}) and "from" (η_{out}):

$$\eta' = \eta_{\text{max}} \eta_{\text{out}} = \frac{\left(1 + \frac{h}{h_0}\right)^4}{n^2 \left(1 + \frac{1}{n} \frac{h}{h_0}\right)^4}. \quad (36)$$

where $n = \frac{n_1}{n_0}$ is the relative refraction index at the boundary of the two media.

We note that (36) was obtained for the field of a point source located at the point where the antenna is located (direct signal focusing) or at the point where the fictitious source is located for the reflection case (reflected signal focusing). The radiator or brightness is assumed to be the same in nonhomogeneous and homogeneous media. The focusing factor η' does not consider the variation of the effective reflecting surface of the object which may occur with replacement of the real nonhomogeneous medium by a homogeneous (reference) medium.

We note also that the magnitude of the focusing factor will depend on the geometric characteristics of the reflecting surface. The variation of the effective reflecting surface of some objects

located in a nonhomogeneous medium was analyzed by Trepov. Figure 7 shows curves of n' as a function of the ratio h/h_0 for reflection from a point target in accordance with (36), from a mirror surface, and from a scattering surface located in the far zone in relation to the radar.

Analyzing these relations, we can say that in the case of vertical sounding of a medium from air the contribution of the focusing factor to the overall radar signal attenuation is not always significant. In all cases it lies in the limits from $-20 \lg n$ to $+20 \lg n$, which for sounding of ice from air varies from -5 to $+5$ dB. However, there is no doubt that the dependence of the focusing factor on the ratio h/h_0 is one of the reasons for the strong dependence observed in practice of radar signal attenuation on airplane flight altitude in radar measurements of glacier thickness. It is precisely for this reason that glacier sounding is usually conducted from low altitudes.

Scattering.

Let us examine radar signal attenuation as a result of scattering of its energy at the upper boundary of and in the medium being studied. In practice two problems arise: one is accounting for the influence of scattering on the overall radio signal attenuation during sounding of the medium, the other is evaluation of the magnitude of the signal "back" scattered by the surface irregularities and the nonhomogeneities within the medium, since this signal is noise when measuring the glacier thickness and may mask the useful signal reflected from the bed.

Usually the scattering capability of the medium is characterized by the scattering index ζ and the scattering indicatrix $\chi(\gamma)$, which are defined by the relations:

$$\zeta = \frac{dP_p}{dP_{\text{max}}}; \quad \chi(\gamma) = \frac{P(\gamma)}{\zeta}.$$

where P_{max} and P_p are the powers incident in the volume dV and

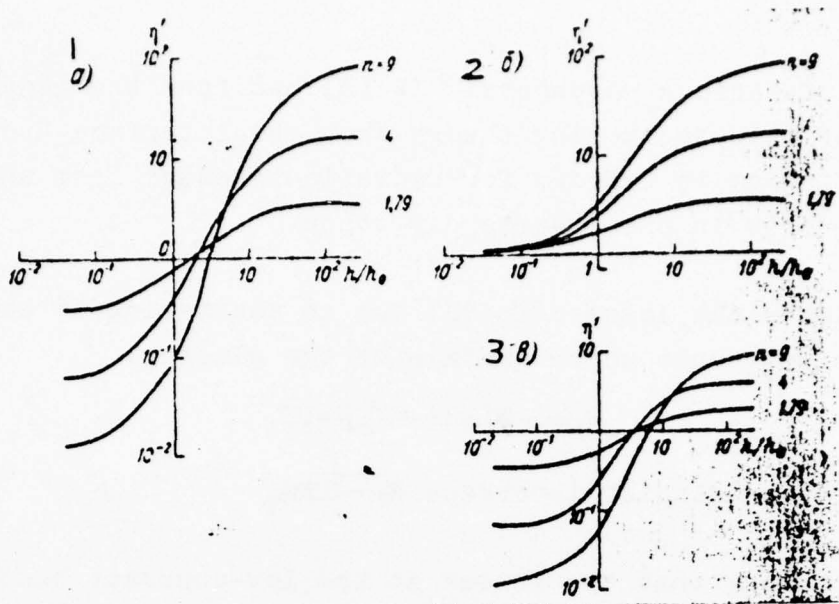


Figure 7. Variation of focusing factor n' with reflection of radio signal from point target (a), from mirror surface (b), and from scattering surface in the far zone (c). 1- a, 2- b, 3- c.

scattered by this volume in all directions; $\rho(\gamma)$ is the power scattered in the unit solid angle in the direction forming the angle γ with the incident wave direction.

Given these characteristics and the absorption coefficient of the medium, the "forward and back" scattered field can be determined by solving the transport equation [19]. These characteristics have not yet been studied in the rf band for snow, firn, and ice, and therefore exact solutions of the problems indicated above are not possible at the present time.

An approximate estimate of the attenuation caused by scattering in a medium can be based on the fact that the considered media have a stratified structure with approximately parallel layer boundaries. In certain cases (water layer in a glacier, thawed soil layer in permafrost) the attenuation caused by scattering may be significant. The signal attenuation resulting from scattering at the upper boundary can be taken into account approximately by the Fresnel coefficient, since for small incidence angles the reflection coefficient is

independent of surface roughness. It follows from the general principles of wave scattering theory that the interface "forward" scattering diagram is broader for radiation passage from the medium into the air than in the reverse direction.

We estimate the losses (in dB) due to scattering as the losses in passage through the upper surface of the glacier:

$$N_s = -20 \lg (1 - K_s^2) = 0.7,$$

where for the air-glacier interface $K_s = 0.284$.

It is obvious that the losses at the low-contrast boundaries of the density nonhomogeneities in the glacier will be still smaller and can be excluded from consideration.

Polarization Losses.

It is well known that if we study an electromagnetic wave with linear polarization in an isotropic medium (air, for example), the signal received from a reflecting object will be maximal when the receiving dipole is parallel to the radiating dipole (provided the depolarizing properties of the interfaces are not significant). In other words, an isotropic nongyrotropic medium does not have depolarizing properties.

It was discovered by the 14th SAE that the signals reflected from the glacier bed have polarization differing from that of the radiated signal. Thus, with linear polarization of the radiated signal the reflected signals have elliptic polarization (linear in particular cases), and the direction of the long ellipse axis does not as a rule coincide with the direction of the radiated signal vector E . We can suggest the following mechanisms of signal depolarization during its vertical propagation in the glacier.

The first mechanism consists in anisotropy of the electromagnetic properties of the ice crystals. It is well known that for monocrystal-

line freshwater ice the difference in the refraction coefficients of the extraordinary (n_{neob}) and ordinary (n_{ob}) waves at the 10 KHz frequency amounts to 0.31 ($n_{neob} - n_{ob} = 5.00 - 4.69$), while in the optical band $n_{neob} - n_{ob} = 1.314 - 1.309 = 0.005$. It is also known that the crystals in the glacier may have an ordered arrangement, specifically: the crystal optical axis is normal to the shear plane of the glacier as it moves.

Depolarization of the propagating wave can arise in those cases when the wave propagation direction does not coincide with the crystal optical axis direction. In this case the depolarization is explained by the fact that the radiated wave is split by such a medium into quadrature ordinary and extraordinary waves, propagating with different phase velocities. In the general case the received signal has elliptic polarization, and linear polarization is possible only if the difference in the ordinary and extraordinary wave phases at the reception point is a multiple of π .

Another explanation for the polarization change is the Faraday effect, the essence of which is that in certain media with the presence of a magnetic field coinciding with the wave propagation direction the propagating wave remains linearly polarized but the polarization plane changes. If the magnetic field direction is perpendicular to the wave propagation direction, depolarization also shows up. However in our case the explanation of depolarization by the Faraday effect cannot be accepted because of the small magnitude of this effect.

There is still another mechanism which can cause depolarization - the stress state of the medium. It is well known that certain substances, specifically glass, in the presence of internal stresses have tensor properties which are not associated with the crystalline structure. The role of this mechanism in the glacier is quite difficult to picture and evaluate because of the little study which has been made of it.

Experiments directed toward study of the laws governing signal polarization variation in vertical radar sounding have been carried out by each SAE, beginning with the 15th. Several different series of measurements have been made and have shown that the polarization diagrams of the received signals are different for different radiating dipole positions. With a certain position of the radiating dipole (in the horizontal plane) we observe minimal signal depolarization - the reflected signal has minimal ellipticity and the polarization plane is rotated very little or not at all relative to the radiated signal polarization plane.

In certain experiments the problem was posed of establishing the polarization autocorrelation radius (at least with respect to received signal polarization plane rotation). The experiments showed that the polarization of signals with different time lag in the general case is different; for the signal with constant time lag the polarization fluctuations with respect to polarization plane rotation angle are small. For example, for one survey line at a distance of 20 meters with average rotation angle 35° the fluctuation amplitude was about ± 5 to $\pm 7^\circ$. We note that the degree of depolarization (increase of ellipticity and change of the rotation angle) is larger, the greater the glacier thickness.

Alteration of signal polarization by the glacier is already used in practice. By using crossed dipoles we can reduce the fluctuations of the signals reflected from the glacier bed and attenuate the signals reflected from nonhomogeneities in the upper, most nonuniform layer of the glacier. The use of crossed dipoles in the 15th and 16th SAE gave tangible results. Study of this interesting phenomenon is continuing.

Some Results of Experimental Studies of Overall Attenuation.

On the basis of the above discussion we can conclude that the quantitative estimate (in decibels) of overall radio signal attenuation as a function of the radar parameters and state and structure of

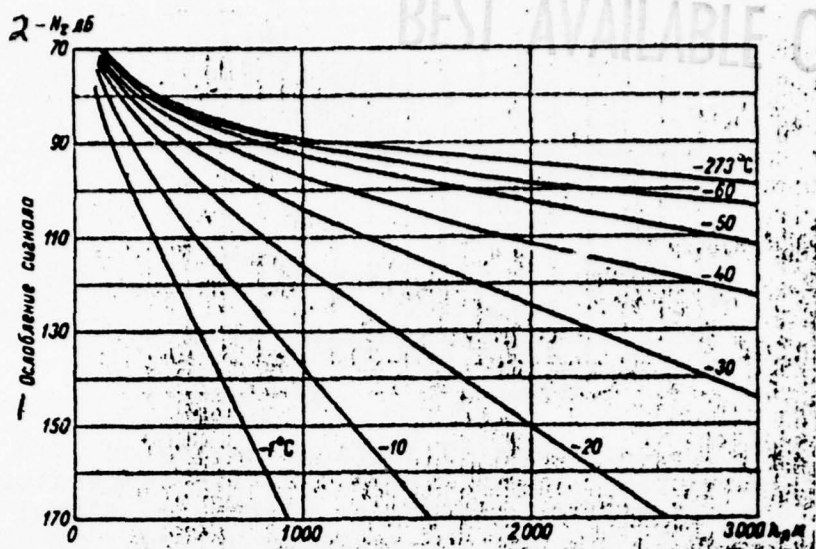


Figure 8. Theoretical dependence of overall radio signal attenuation on glacier thickness for different absorption temperatures.
 1- signal attenuation; 2- dB.

the glacier can be made using the formula:

$$N_e = -20 \lg \sigma \lambda + 20 \lg k + N_s(t_g) k + 40.7 \quad (37)$$

where the quantity 40.7 dB, defining the scattering, focusing, and depolarization losses, may change for specific conditions.

The results of N_e calculation using (37) are shown in Figure 8. Figure 9 shows the experimental data on the influence of surface thawing on signal level in radar sounding. We note that the large signal attenuation increase which is recorded experimentally upon melting of the glacier cannot be explained by the reflection coefficient increase alone. Thus, even a quarter-wave water layer ($\epsilon'' = 81$) on a snow surface ($\epsilon''_{ch} = 2$) has reflection coefficient K_{fl} equal to 0.965, which leads to upper boundary reflection losses N_p of approximately 23 dB.

The overall attenuation is in general a random quantity (see Section 6). This is clearly confirmed by the reflected signal

BT AVAILABLE COPY

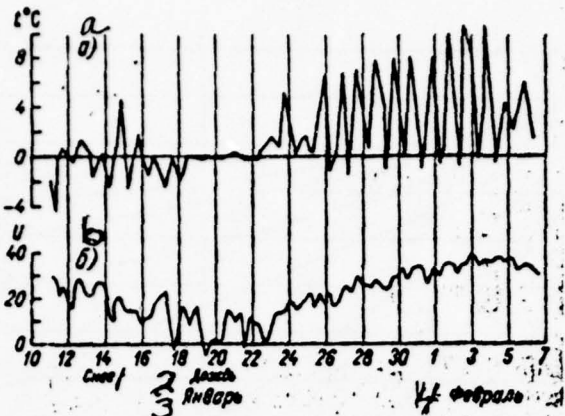


Figure 9. Influence of surface thawing on reflected radio signal level. a) air temperature in the observation period; b) voltage of signal reflected by the bed (in relative units).
1- snow; 2- rain; 3- Jan.; 4- Feb.

fluctuations. Nevertheless the large number of overall attenuation measurements makes it possible to perform averaging and verify the validity of the adopted theoretical model for various conditions (glacier thickness, glacier average annual temperature, equipment parameters). The contribution of the individual components of $N\epsilon$ can be determined by special experiments.

Unique studies were made in the 14th SAE to determine the overall signal attenuation frequency dependence. The experiments were made using a specially developed radar set having frequencies of 60, 70, 100, 140, 200, and 400 MHz. The experiments confirmed the validity of the adopted radio signal propagation model when sounding glaciers. In accordance with this model we can calculate the geometric losses using the $1/h^2$ law, and the focusing factor and the losses in reflection from the glacier bed can be calculated as indicated above. The losses resulting from scattering for cold glaciers are about 1 dB and increase to 20 - 30 dB with thawing of the surface layer.

To calculate the absorption magnitude we need to know the absorption temperature, which can vary from 0.75 to 0.9 of the annual

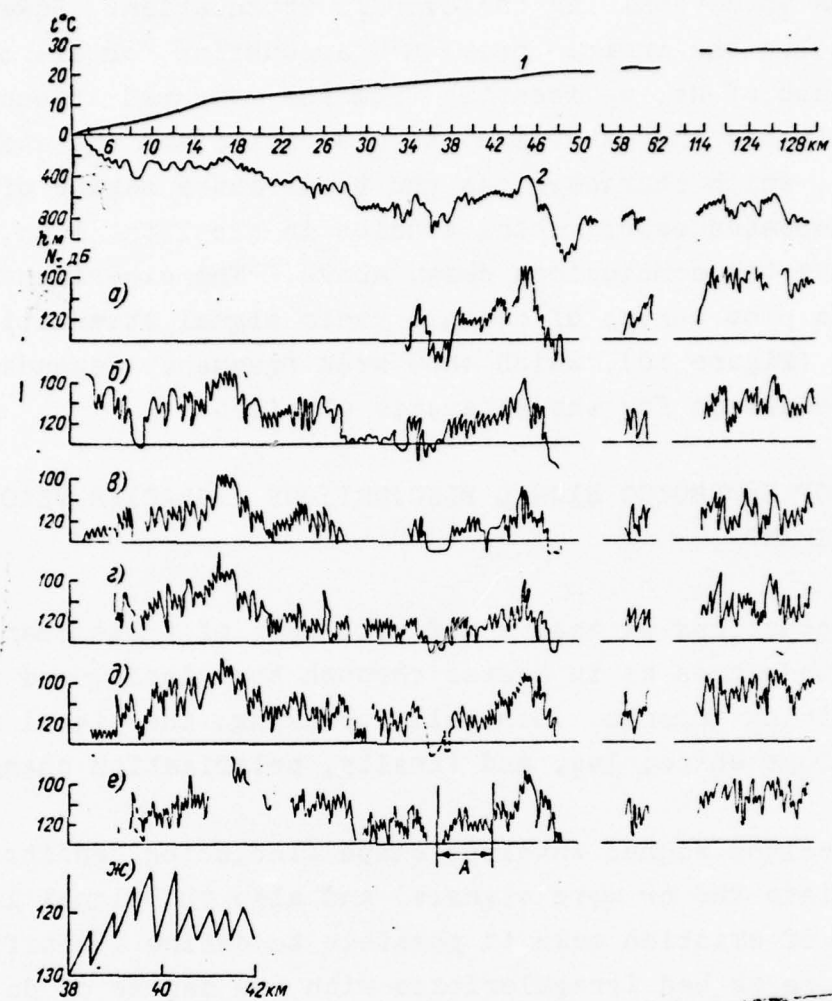


Figure 10. Averaged overall attenuation of radio signals of different frequency along a single measurement line. a) 60 MHz; b) 70 MHz; c) 100 MHz; d) 140 MHz; e) 200 MHz; f) 440 MHz; g) attenuation of radio signal on segment A (to enlarged scale); 1) annual average air temperature along line; 2) glacier thickness: horizontal scale is distance south of Molodezh Station.

average air temperature near the surface, which does not lead to large errors in determining the overall attenuation. However it is better to solve the inverse problem: accounting for all the remaining components of $N\epsilon$, we identify from the measured attenuation the absorption losses and determine the absorption and the absorption temperature, which characterizes the temperature regime of the glacier. Repeated experimental studies in the 15th, 16th, and 17th SAE confirmed the conclusions drawn above. The experimental data were used to plot curves of overall radio signal attenuation for six frequencies (Figure 10), which show weak frequency dependence of the overall attenuation for the Antarctic glaciers.

6. STUDY OF REFLECTED SIGNAL FLUCTUATIONS. GLACIER VELOCITY MEASUREMENT

By fluctuations we mean a definite part of those changes which the signal undergoes as it passes through the glacier and returns to the receiving antenna. Generally speaking, the signal amplitude, phase, envelope shape, lag, and finally, polarization change.

The received signal envelope shape (including "splitting" of the signal into two or more signals) and also the signal lag relative to the time of emission make it possible to define stratified glacier structure or bed irregularities with the degree of detail provided by the radar range and angle resolution and also make it possible to determine the depth at which these irregularities lie. When using a radar with signal detection we do not observe phase changes.

In the case of matched polarization of the transmitting and receiving dipoles the signal amplitude varies regularly with increase of the glacier thickness and variation of its temperature and randomly with respect to many factors, unambiguous identification of which is not possible at the present time.

In this section we shall analyze the random component in the

signal amplitude variation which is determined by the different influence of scattering at the glacier surface and at its lower boundary, by the polarization change, by the difference in absorption in micrononhomogeneities, and so on. Use of amplitude samples obtained in accordance with the Kotel'nikov theorem ($T \leq T_s$, amplitude recording interval T shorter than the stationary random process high-frequency component T_s period) detailed statistical analysis of the amplitude fluctuations. This analysis is important in solving several practical problems. For example, knowledge of the autocorrelation radius R_a makes it possible to evaluate the effectiveness of weak signal energy accumulation when sounding a glacier from carrier vehicles traveling comparatively slowly with respect to the glacier and from a fast-flying airplane.

Photographic recording of the reflected radio signal fluctuations was first accomplished by the 16th SAE (January, 1971). Recording was accomplished at three frequencies (60, 213, 440 MHz) from a slowly moving vehicle on segments whose lengths in the various experiments were 20 - 100 M. The recording frequency was 200 - 250 frames per 100 meters of survey line. Signal amplitude was displayed using type A scan. Since the electromagnetic signal alters its polarization as it propagates in the glacier, and since the nature of the sub-glacier bed is probably different in the direction of glacier flow and in the perpendicular direction, the measurements were made along lines arranged in the form of a cross. Figure 11 shows the reflected signal amplitude as a function of distance. The large amount of experimental data on reflected signal fluctuation was machine processed. For this purpose the filming interval was first normalized (the vehicle travels at different speeds in different series of measurements). The computer was used to calculate the autocorrelation relations for the signals of the three frequencies for all the survey lines and measurement points and the cross-correlation relations of the fluctuating signals of different frequencies along the same survey line.

Analysis of the reduced data made it possible to determine the

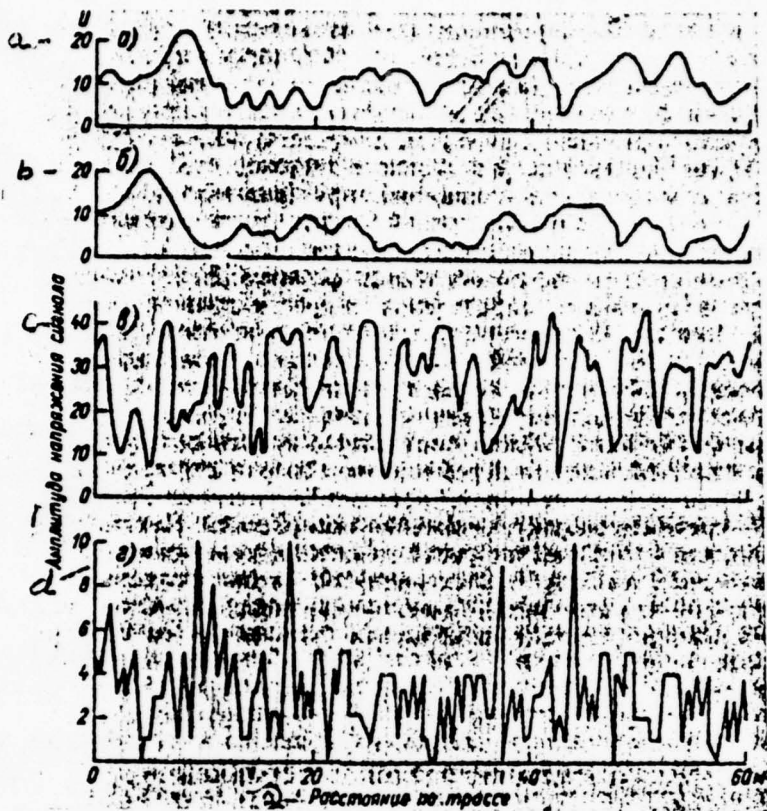


Figure 11. Fluctuations of radio signals reflected by bed. a, b) at 60 MHz for two mutually perpendicular directions with $R_a = 5.2$ and 5.1 m respectively; c) at 213 MHz with $R_a = 1.6$ m; d) at 440 MHz with $R_a = 0.8$ m. 1- signal voltage amplitude; 2- distance along track.

fluctuation autocorrelation radius. For the 60 MHz frequency the autocorrelation radius is approximately $5.1 - 5.2$ m, for the 213 and 440 MHz frequencies it is 1.6 and 0.2^8 m respectively. It was also established that the scattering properties of the glacier bed are the same for different measurement survey line orientations; the fluctuation pattern is more stable, the lower the frequency and the greater the glacier thickness.

The data of statistical analysis of the signal fluctuations indicate the possibility of determining glacier surface velocity

relative to the fluctuation pattern fixed with the bed. For this purpose it is necessary to make repeat measurements of the fluctuations on the survey lines with some time interval. If we then superpose the fluctuation diagrams obtained at different times we can determine their relative shift, which is proportional to the glacier surface displacement and finally, considering the time interval between pictures, we can determine the average surface velocity. We assume that the surface velocity measurement accuracy will amount to a fraction of the aforementioned correlation radii. We emphasize that this method makes it possible to measure the glacier velocity in regions far from exposed rock formations.

7. RADIOINTROSCOPY OF GLACIERS

By glacier radiointroduction we mean study of the internal structure of glaciers with the aid of radio waves. The primary elements of glacier microstructure are its layering, presence of foreign inclusions in its interior, continuity of the cover, and structure of the lower boundary of the glacier, which is in contact with the bed.

Study of Glacier Stratified Structure and Foreign Inclusions.

We mentioned previously that glaciers have three primary layers: snow, firn, and ice. The radar method makes it possible to study the nonhomogeneity of these layers and detect foreign inclusions in the glacier, for example, moraine-bearing strata.

Two types of reflecting nonhomogeneities are possible in the interior of the glacier: layers with different glacier material density or different crystalline structure, and the ice layers which contain rock inclusions - moraines. Two groups of reflected signals correspond (on the oscillograms or in time) to these nonhomogeneities: one is near the sounding pulse and the other is near the pulse reflected by the bed. We note that reflected signal interpretation is very difficult; a special technique and specially planned experiments and processing of the results are required. In some cases the

reflected signals may indicate the presence of moraine-bearing layers near the bed. For example, sounding near a borehole in the Mirnyy Observatory region showed that the glacier thickness here is 120 meters, however a reflected signal was also received from a depth of about 80 m. Later, morainic material was detected during drilling in the ice at a depth of 75 m, drilling was terminated because of the presence of this material.

We shall present some other examples.

In the 12th SAE during simultaneous sounding of the glacier at frequencies of 100 and 440 MHz layered glacier structure was recorded at a distance of 30 - 80 meters from the glacier bed. In 1971 during the 16th SAE a radar operating at 440 MHz detected on a survey line passing to the south of Molodezh Station a nonhomogeneity layer about 5 km long, lying at a depth of about 1000 m, approximately half the glacier thickness.

Radiosounding of the glacier from an airplane on a route from Molodezh Station along the meridian of this station at 72° S, and then after a turn to the Japanese Syov Station, and from there back again to the Molodezh Station gave unique results. Signals whose time lag relative to sounding pulse is greater than the lag of the signals reflected from another interface lying below the glacier bed were recorded. It is believed that this interface is the freezing boundary of the bedrock located beneath the glacier. It should be noted here that correct interpretation of the signals received from nonhomogeneities in a glacier is aided significantly by observations with the aid of boreholes, observations of the glacier face along the coastline, and also inverted icebergs.

Detection of Hidden Crevasses.

The detection of crevasses hidden by snow bridges is a very important problem, since its successful solution makes it possible

to ensure safety of vehicle movement on crevassed glaciers.* Evaluation of ice massif continuity on areas selected for takeoff and landing strip construction is also very important. Radar crevasse finders not only facilitate considerably the selection of such areas, but also make possible continuous monitoring of their condition. An attempt was made in the 12th SAE to detect crevasses from an airplane by radar. The experiments showed that the signals reflected from crevasses located at distances up to four kilometers are easily tracked during flight at 300-meter altitudes. This showed that the signals reflected from crevasses can be detected with small rf wave glance angles (relative to the glacier surface).

For detecting and determining the location and orientation of crevasses, and also for measuring their width, it is best to use perspective sounding or panoramic radar scan from a surface vehicle or an airplane.

The overall attenuation of the signals reflected from crevasses when using perspective glacier radiosounding can be calculated using the general scheme presented in Section 5. It is obvious that for detection and exact determination of crevasse location and dimensions, it is necessary to use equipment with better spatial resolution than in the case of glacier thickness measurement, for example, with radiation pattern width 10° and pulse duration 10 ps. However the first attempts to detect crevasses by the panoramic radar scan method from a surface vehicle were made with the aid of the very simple RV-10 equipment, which is used for vertical sounding.

The effective reflecting surface area of glacier crevasses and the backscatter diagram have not yet been studied. Therefore for

* Crevasses arise basically because of nonuniformity of glacier movement. Their depth reaches hundreds of meters and they are covered over by snow bridges. During the first radiosounding experiments the tractor-sled train broke through into a crevasse 22 meters deep.

an approximate evaluation we can consider the crevasse to be a plane layer with rough boundaries. The irradiated crevasse segment area (in m^2) in the limits of a single radar spatial resolution element can be determined from geometric considerations using the following expression:

$$s_r = \frac{c_s \tau_{\text{max}}}{2} \cdot \frac{1}{\cos \alpha} \sqrt{R \frac{c_s \tau_{\text{max}}}{2}},$$

where α = glance angle in relation to the crevasse plane; R = distance to crevasse.

Trepov gave the parameters of the equipment used for the experiments and presented the necessary calculations, based on account for the radio signal attenuation components in perspective sounding for the case with antenna located 8 meters above the glacier surface. When using radar with frequency 440 MHz ($G = 2$; $\tau_{\text{max}} = 0.3 \mu\text{s}$, potential 130 dB) signals reflected from crevasses can be detected at distances over 100 meters and when using radar with frequency 3000 MHz ($G = 300$, $\tau_{\text{max}} = 10 \text{ ns}$) and the same potential they can be detected to nearly 100 meters.

The problem of radar detection of crevasses is complicated by the presence of noise in the form of signals reflected from irregularities on the glacier surface (sastrugi) and nonhomogeneities in the upper part of the glacier. The level of this noise is determined by the glance angles, antenna pattern width, degree of surface irregularity, and density nonhomogeneity of the glacier. Experiments are required to evaluate the noise level.

Experimental studies were made during the 14th SAE to clarify the possibilities of using perspective radar sounding for crevasse detection in glaciers. The sounding was made with the aid of the RV-10 radar. The indicator was an SI-20 oscilloscope. The receiving and transmitting antennas were mounted on a mast on the roof of the mobile laboratory at a height of 7 - 8 meters above the glacier surface. The studies were made near Molodezh Station on the airfield and the glaciological test range, and also in the crevasse zone near

Sibiryachka Bay (March, 1969). The oscillograms show a significant reflected signal level at distances 0 - 300 M when sounding in the crevasse zone and practically no signal in regions with monolithic ice (airfield). It was noted that the reflected signal level is considerably higher with the antenna oriented perpendicular to the crevasses than with orientation along the crevasses (Figure 12).

Thus the radar signals reflected from crevasses are observed reliably on the perspective sounding radar screen. However, because of the low spatial resolution of the equipment used, it is rarely possible to establish unique correspondence between the radar signals and crevasse location in the glacier. The use of equipment with higher spatial resolution will obviously make it possible to solve this problem. Modified equipment was tried out in the 18th SAE (1973). Experiments on perspective crevasse sounding were made at 440 MHx frequency with use of an antenna array consisting of eight radiators with a flat reflector. This equipment was developed by the radiophysics division of the Arctic and Antarctic Scientific Research Institute (AANII) in 1972.

Study of Glacier Bed Relief.

The relief of the lower boundary of the glacier is completely identical to the relief of the underlying bedrock. Therefore study of the structure of the relief of the lower, bottom surface of the glacier reduces to study of its sub-ice relief.

Study of the sub-ice relief was initiated by the 10th SAE and is continuing at the present time. The results of the studies are used by the Division of Aerial Photography and Cartography of Soyuzmorniiproekta and by the Division of Geography of Polar Countries of AANII for mapping the sub-ice relief. Recording of the sub-ice relief includes measurement of airplane altitude relative to sea level (H_a), radar measurements of flight altitude above the glacier (H_{pa}), and radar measurements of glacier thickness (h). These data are used to calculate the position of the glacier surface ($h_a = H_a - H_{pa}$) and the glacier bed ($h_x = H_a - H_{pa} - h$) relative to sea level.

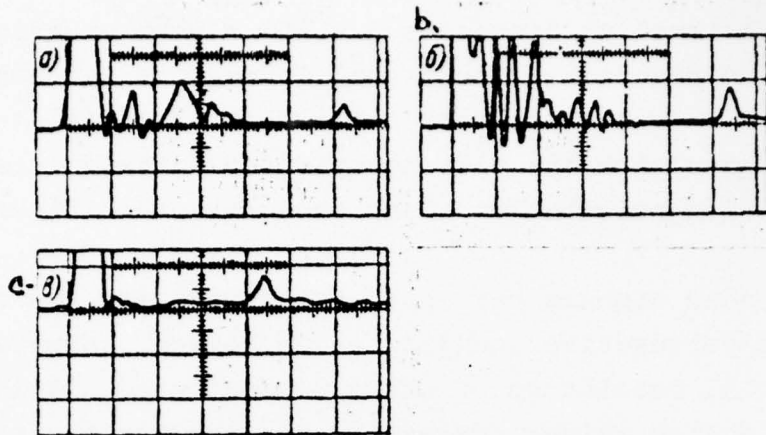


Figure 12. Oscillograms of perspective glacier radiosounding. a) sounding in crevasse region near Sibiryachk Bay, antenna oriented along crevasses; b) same, antenna oriented across crevasses; c) sounding in region without crevasses (airfield, Molodezh Station). The signal reflected from the glacier bed is seen on the right side of the oscillograms.

The radiosounding survey line is "referenced" to the map on the basis of airplane navigational instrument indications and data of aerial photography of the point of airplane approach to the sounding line from the coastline and the point of departure from the pass.

The degree of detail of the sub-ice relief record is very high (frame-by-frame recording of the radar screen is accomplished approximately every kilometer). This detail makes possible more precise analysis of certain characteristic features of the sub-ice relief and permits more valid generalization of the data than is possible when using a large-scale map prepared on the basis of radiobarometric surveying. At the present time radar surveying has been performed on routes whose overall length is more than 100,000 KM. The routes cover an area of about one million square kilometers.

The most characteristic and prominent feature of the sub-ice relief of the part of Antarctica which we have studied is its irregularity; we frequently encounter depressions and peaks whose base

width is equal to or somewhat greater than their vertical dimension. This contradicts the concepts on the basis of which the existing map of the sub-ice relief of Antarctica was drawn [2].

The radiobarometric survey data led to the detection of a "sub-ice" strait, extending from Edward VIII Bay to Amudsen Bay, a large mountain massif to the south of this "strait" between 68 and 69.5° S, a sub-ice mountain lowland adjacent to the Syov Station, a second large mountain massif to the south of Syov Station, extending southward from 72° S latitude.

In the 17th SAE (1972) a detailed area-type survey of the sub-ice relief was conducted in a special tractor-sled expedition. Two test ranges were selected for this purpose on the Mirnyi-km 153 route in the direction of Pioner Station. These test ranges had areas of $5 \times 5 \text{ KM}^2$ and were located at km 57 and km 153 of the indicated route. Radiosounding was accomplished by surveying the test ranges along mutually perpendicular lines at intervals of 500 meters.

The survey made on these test ranges not only made it possible to obtain detailed two-dimensional maps of the sub-ice relief, but also made it possible to "tie in" to the bed relief the test range points marked by stakes.

Figures 13 and 14 illustrate the work done in studying the spatial structure of the lower boundary of the glacier. Repeat surveys on these test ranges will make it possible to evaluate glacier displacement relative to the "bottom" reference points.

In conclusion we note that radiosounding makes it possible to obtain the very detailed information which is necessary for map preparation and geologic study of the bedrock.

BEST AVAILABLE COPY

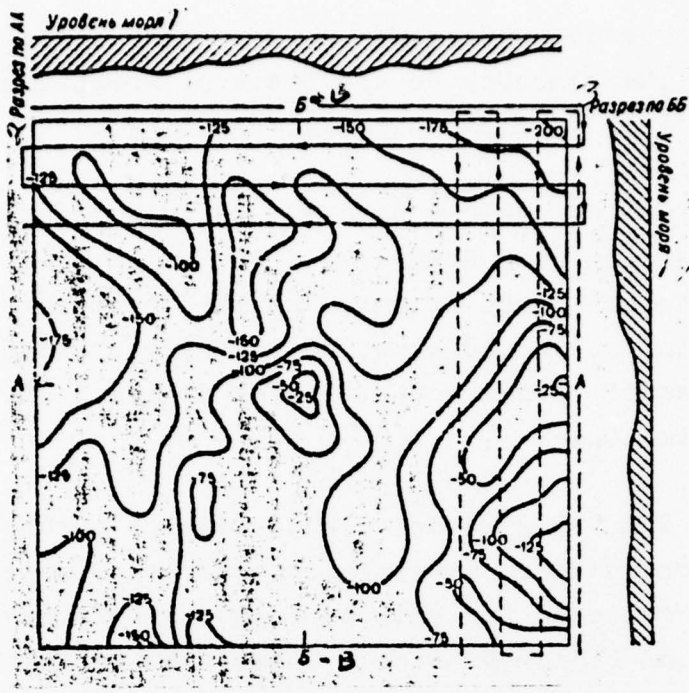


Figure 13. Sub-ice relief (meters) on test range No. 1. The straight lines indicate the sounding routes. 1- sea level; 2- section AA; 3- section BB.

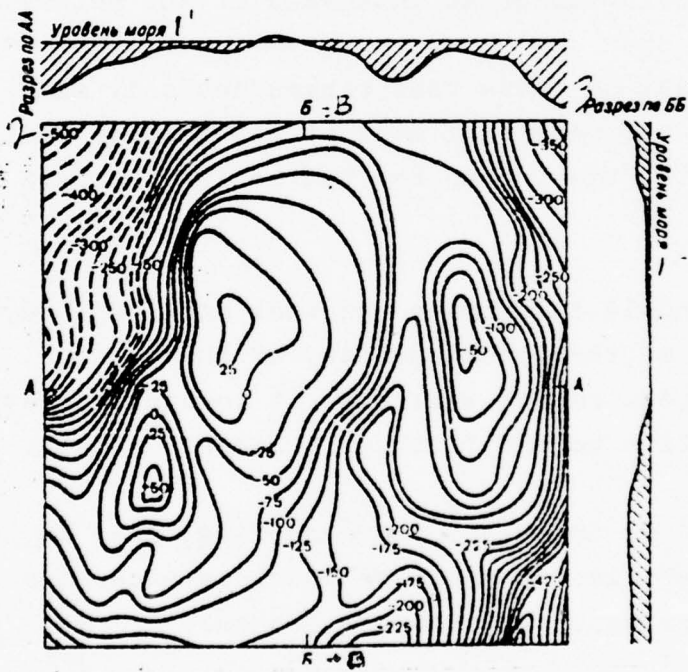


Figure 14. Sub-ice relief (meters) on test range No. 2. 1- sea level; 2- section AA; 3- section BB.

8. RADIOSOUNDING OF TEMPERATURE AND MOUNTAIN GLACIERS

Characteristics of Glacier Structure and Properties.

We have discussed the theoretical and experimental studies directed toward the development and introduction of radar methods for extensive study of the cold glaciers of Antarctica. Radio-sounding of the Arctic (temperate) and mountain glaciers is also of great practical interest. The radar methods are without question the most precise and fastest and can be used to evaluate the water resources of these glaciers and study their physical characteristics.

The temperate and mountain glaciers differ markedly from the Antarctic glaciers in their properties: their average interior temperature is higher and sometimes close to 0°C , on the glacier surface there is nearly always a layer of wet snow or water, within the glacier there are layers of different density corresponding to the annual cycle of glacier mass accumulation and layers of foreign matter due to rock formation weathering. The specific properties of the mountain glaciers make the radar method in the form in which it is used in Antarctica ineffective for measurement of the thickness of these glaciers.

It is well known that electromagnetic wave dielectric losses increase markedly with increase of the ice temperatures to values close to 0°C . Table 7 presents the energy absorption of a plane wave as it propagates over a distance of two kilometers (glacier thickness one kilometer). The layer of wet snow or water on the surface of the thawing glacier leads to significant reflection from the air-ice interface in comparison with the dry glacier case. While at the air-ice interface the reflection coefficient is 0.28, with a quarter-wave water layer present on the surface of the ice the coefficient is 0.92 (without account for the dielectric losses).

TABLE 7

Frequency, MHz	440	200	100	60	30	10
Absorption, dB						
at -1° C	102.4	97.8	91.2	87	81	70

at - 20° C About 30

Increase of the attenuation of the 440 MHz frequency radar signal upon glacier thawing was demonstrated experimentally in the 11th and 12th SAE: with a wet snow layer 10 - 15 CM thick present the attenuation was 20 - 30 dB. The signal attenuation because of reflection from layers differing in electrical properties (different ice density, rock inclusions) depends on the glacier structure. According to measurements made in the 12th SAE (1967) at this same frequency the attenuation is only a few decibels for the Antarctic glaciers. For the more nonhomogeneous mountain glaciers the attenuation because of internal reflections is considerably higher. With the presence of periodic layers commensurate in thickness with the wavelength the attenuation may reach tens of decibels.

From comparison of the overall radio signal attenuation in mountain and Antarctic glaciers, we can conclude that the radar with carrier frequency 440 MHz and receiving channel sensitiviey 130 dB relative to the peak transmitter radiated power can measure mountain glacier thickness reliably to 80 - 100 M. Considering that mountain glacier thickness reaches 300 meters or more, lower frequencies (10 - 100 MHz) should be used.

Another characteristic of mountain glaciers is the marked irregularity of their surface. In this connection reflections from their surface irregularities are possible when radiosounding such glaciers. These reflections made identification of the useful signal difficult. Highly directive antennas must be used to reduce the interfering reflections.

Calculation shows that the radar set with receiver sensitivity 150 dB relative to the peak transmitter power, carrier frequency 60 MHz, and 10 dB gain antenna can provide mountain glacier thickness measurement to within 300 - 400 M.

Radiosounding of Soviet Arctic Glaciers.

In 1968 the Sever-20 High-Latitude Expedition conducted the first experiments in the U.S.S.R. on radiosounding of the Severnaya Zemlya Archipelago glaciers [11]. English and American scientists made similar studies in 1966, performing airborne radar measurements of glacier thickness on Ellsmere Island.

The arctic glaciers have comparatively small dimensions and many landmarks are available in the periglacial zone. Therefore aerial photography makes it possible to obtain precise tie-in of the sounding survey lines. The Severnaya Zemlya Archipelago glacier thickness does not exceed 1000 meters. The regional glaciological conditions and the meteorological characteristics of certain regions of the Arctic require selection of the most suitable time of the year for sounding, when meltwater is not present in the upper glacier layers, the weather is sunny, the downslope winds are minimal, and consequently low-altitude flights above the glacier are safest. The limited time with favorable weather conditions in the period in which the fore-mentioned experiments were conducted shortened the duration of the studies and therefore not all the most characteristic Severnaya Zemlya Archipelago glaciers were studied equally thoroughly. Figure 15 shows a schematic of flights made for glacier radiosounding. We see from the figure that radar thickness measurements were made on the glaciers of Schmidt, Komsomolets, Pioner, Oktyabr'skoe Revolyutsii Islands, forming the Severnaya Zemlya Archipelago, and on the glacier of Ushakov Island, located in the Kara Sea to the northwest of this archipelago.

A radar with the following characteristics was used for the radiosounding:

BEST AVAILABLE COPY

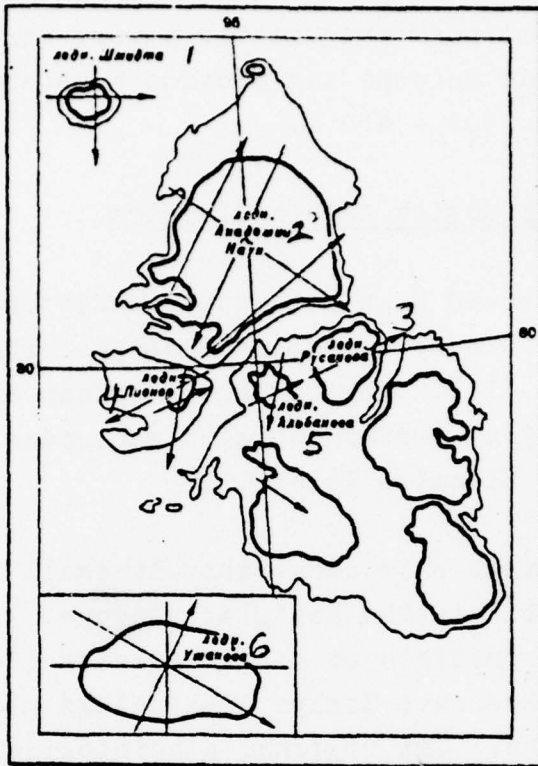


Figure 15. Diagram of flights made in radiosounding Severnaya Zemlya Archipelago glaciers. 1- Schmidt G.; 2- Academy of Sciences G.; 3- Rusakov G.; 4- Pioner G.; 5- Al'banov G.; 6- Ushanov G.

Carrier frequency $f = 100$ MHz
Pulse power $P_{\text{pulse}} = 5-7$ W
Pulse duration $\tau_{\text{pulse}} = 0.3$ μ s
Receiver sensitivity $P_{\text{rec}} = 5 \cdot 10^{-13}$ W

Separate "double square" antennas, located on the fuselage of an Li-2 airplane in the wing region and spaced two meters from one another, were used to radiate and receive the signals. The flight altitude above the glacier surface was measured by this same radar. Barometric measurements were made in order to reference the air-glacier, air-rock formation, and glacier glacier-bed interfaces to sea level. The barometric altimeter indications were "referenced"

to sea level in the regions of approach to the coastline and departure from the coastline based on the airplane radio-altimeter indications. The measurements were recorded by an automatic photocamera.

It seems to us that the best time of the year for radar sounding of Arctic glaciers is spring (March, April, early May). In this period, glacier thawing is still not marked and electromagnetic wave energy absorption is not significant. Another important factor are the long periods of sunny weather -- they ensure flight safety at low altitude above the glacier. The studies undertaken by the Sever-20 expedition made it possible to obtain important information on thicknesses of the glaciers studied with error no more than -7, + 3%, define more exactly the glacier bedrock location in relation to sea level, and evaluate the relief of this bedrock.

Radar signal attenuation calculations showed that during conduct of the measurements the electromagnetic signal losses in the glacier due to absorption do not exceed those for the continental Antarctic glaciers in the 10 - 15 kilometer zone along the coast. All the glacier thickness data are summarized in the tables of [11].

9. RADIOSOUNDING OF SEA AND FRESHWATER ICE

By radiosounding of sea and freshwater ice, we mean remote determination of the thickness and study of the structure of the ice covers of various water bodies with the aid of active radar methods. We believe that this problem was first formulated in [7]. However the practical use of the results of that study, obtained for simplified models of freshwater ice, was limited.

The importance of developing a reliable remote method and radar equipment for sounding floating ice covers is obvious. Expansion of the commercial transport volume in the Arctic, study and practical use of the Arctic sea shelf, navigation in the northern river estuaries, scientific prognosis of ice conditions -- all these are very important economic problems. Their successful solution requires methods for

fast collection of data on the ice cover thickness over large areas. The availability of such hardware aboard the airplanes used for ice scouting and navigation support, and also aboard the helicopters of the icebreakers, would broaden markedly the information on ice cover status in their operating zone and would facilitate the selection of ship navigation and maneuvering tactics.

It is well known that the development of radar for sounding the ice covers of different water bodies is a very complex physical and engineering problem. Its complexity is determined primarily by the absence of generalizing electromagnetic characteristics for sea and freshwater ices in the meter to decentimeter wavelength band. The ice covers of water bodies, particularly the Arctic seas, have very complex structure: they include pack, perennial, and young ice of differing thickness. All these different ice varieties have different electromagnetic characteristics, varying markedly across their section as a function of ice age, thickness, and temperature. Therefore statistics on ice cover geometric (dimensional) parameters and a large amount of data characterizing the variability of their temperature and salinity conditions are necessary for optimization of the technical solutions.

It is obvious that particularly important in this problem are reliable data on floating ice cover electromagnetic characteristics (ϵ' and $\text{tg}\delta$) and the physics of the so-called matching layer, at the expense of which ice incrementation takes place. This layer is extremely nonhomogeneous, both as a dielectric and as material of the phase change zone.

There are also definite complexities in the technical aspects. The radar must have high time resolution, high potential, and narrow antenna pattern. In the last three to five years extensive studies have been conducted in several countries and particularly in the U.S.S.R. of floating ice cover electromagnetic characteristics, which have advanced considerably the solution of the problem of developing the radar method for sounding floating and particularly

Arctic drifting ice.

Electromagnetic Characteristics of Sea and Freshwater Ice.

A quite wide frequency band is applicable for sounding sea ice by active radar methods; from 30 to 1000 MHz. In [9] the radar range equation was used to calculate the overall attenuation of electromagnetic waves during propagation in sea ice. The calculation results are shown in Figure 16. In the calculations it was assumed that the Fresnel coefficient of reflection from the lower boundary is equal to one, the ice layer is plane-parallel, and wave incidence is normal. These data show that a radar potential of 140 - 160 dB is required for sounding sea ice. Full-scale experimental data on the magnitudes of the refraction index n and electromagnetic energy absorptivity N_n (dB/m), which determine the wave phase velocity and the required radar energy potential, are necessary for optimal solution of the problem.

At the present time results are already available of laboratory and full-scale measurements of these characteristics. We consider the most reliable measurements to be those made by Khokhlov on the SP-13 drifting station [12] and those made by Tripol'nikov in 1972-73 on the SP-21 drifting station. Khokholov measured ϵ' and $\operatorname{tg}\delta$ of drifting ice in the 100 Hz to 1 MHz band and showed their functional dependence in the anomalous dispersion region on ice salinity, structure, and temperature. Tripol'nikov studied the "quiet" frequency band: 30 - 400 MHz.

Laboratory and full-scale studies of ϵ' and $\operatorname{tg}\delta$ in the 10 Hz to 100 MHz band are discussed in [28-30]. These data do not cover the entire frequency band which we believe to be promising for radar study of sea ice. It should be emphasized that sea ice is a strongly absorbing, stratified nonhomogeneous dielectric which changes its

* By "quiet" we mean the frequency band where ϵ' retains an approximately constant value.

properties sharply under the influence of various inputs and is very difficult to model under laboratory conditions. In addition the technique of these studies is based on measuring the parameters of concentrated chains. For the meter-centimeter wavelength band the estimates of ϵ' and $\text{tg}\delta$ are best made by modeling the wave propagation process in sea ice. In [13] an attempt was made to measure the absorption under full-scale conditions at frequencies of 100, 440, and 1000 MHz. These results do not agree with the data of [28]. In the following we shall discuss the results of full-scale measurements made by Tripol'nikov.

The data of electromagnetic wave propagation velocity and absorptivity measurements in the 30 - 400 MHz band in sea ice were obtained by pulse "sounding" of coaxial long lines having sea ice as the dielectric under study. In such a line in the absence of conditions for resonant energy exchange between the field components E and H the signal attenuation is due basically to losses in the dielectric. In this case the measured specific attenuation can be taken as the maximal estimate of the specific absorption. It will be clear from the quantitative results presented below that when using sea ice as the dielectric in the line the specific attenuation practically coincides with the specific absorption, and the wave velocity in the line coincides with the velocity in the medium. Coaxial lines of length from two to eight meters were used for the measurements.

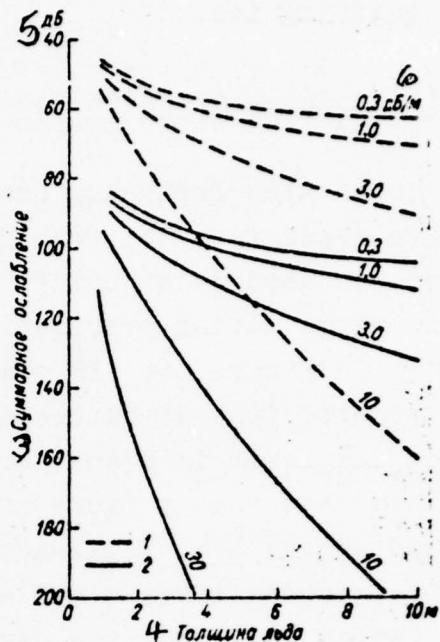


Figure 16. Calculated overall radio signal attenuation in sea ice for various absorptivities. 1- antennas at one-meter height; 2- antennas at 100-meter height; 3- overall attenuation; 4- ice thickness; 5- dB; 6- dB/m.

The measurement technique was developed and the line parameters were optimized under laboratory conditions. Observations were made of the passage of radio signals of duration from 0.05 to 0.5 μ sec with frequencies 30, 60, 100, 200, 400 MHz through lines filled with ice of different salinity, and also video pulses of duration 0.02 μ sec with repetition frequency 10 kHz. The wave propagation velocities were measured on the basis of the delay time of the signal passing through the line. The specific attenuation measurements were made by the variable length line method and on constant-length lines with account for the losses in reflection from the ends of the line. The measurements were made at temperatures from -40 to -5°C. Pulse front distortion was observed with salinity 17% and temperature above the eutectic for NaCl. But since the group velocities coincide for the rf and video pulses this effect can be explained by the frequency dependence of $\operatorname{tg}\delta$.

It was also noted that with temperature increase above -22°C, there is reduction of the velocity, and the more marked the higher the sample salinity. This phenomenon can be explained by the appearance of a liquid phase in the medium under study -- brine droplets, whose concentration in the total ice volume increases with increase of the temperature and salinity. In this case the sounded medium is a mixture of ice and water with some effective ϵ' . This effect is of fundamental importance for correct interpretation of sea ice radar sounding. For example, the annual average temperature of drifting sea ice at a depth equal to half its thickness lies approximately in the range from -5 to -8°C, the salinity of year-old ice at this same level is about 4-5%. For such ice the sounding pulse velocity in the ice can be taken as 140 m/ μ sec. In perennial pack ice the salinity at the 0.5 thickness level is about 0.5%; in such ice the electromagnetic wave velocity is 170 m/ μ sec. The series of laboratory measurements made it possible to evaluate the specific absorption of electromagnetic waves in ice of different salinity and temperature. It was found that ice phase composition variation as a function of thickness can have significant influence on sounding result interpretation accuracy. Therefore it becomes necessary to obtain the

averaged electromagnetic characteristics of sea ice of different age and ice-formation conditions.

We have mentioned previously the need for studying the electrical properties and in general the physics of the matching layer. In the present case it is very important to explain the presence of electromagnetic contrast at the crystallization boundary of sea water. This question is controversial, and for its concretization we shall present some information on sea water crystallization process.

The first ice crystals form upon cooling sea water to -1.9°C . Further temperature reduction facilitates the crystallization process, as a consequence of which the salt concentration in the solution increases. The concentrated solution (liquid phase) which remains in the crystallization process fills either local volumes or inter-crystalline layers, forming communicating channels. At low temperatures the local volumes dominate and at higher temperatures -- the channels. At certain temperatures the solution can become saturated for some component and then this component precipitates. Thus KCl precipitates at -11.1°C , NaCl at -22.6°C . CaCl_2 has the lowest eutectic temperature, it precipitates at -55°C . It follows from this that natural sea ice cannot contain a liquid phase in its structure. The crystallization process leads to capture by the ice crystal lattice of the solution ions. And although their concentration is extremely low the influence of impurities on the electrical characteristics of crystallized ice is very significant. The influence of the liquid phase on the physical properties of sea ice is significant: at not very low temperatures brine occupies a considerable fraction of the total volume. The temperatures of the lower layers of the formed ice cover of thickness about 0.5 meters, covered with a snow layer, are close to the crystallization temperature; they are very strongly, nearly half, saturated with concentrated brine. Therefore it is very important not only to explain the presence of electromagnetic contrast of this unique boundary, but also to estimate its quantitative characteristics for the meter and decimeter wavelength band. We have not found such information in the literature.

Tripol'nikov carried out a major series of studies on the SP-21 drifting station, using the long-line measurement method. This technique made it possible to determine electromagnetic signal attenuation, wave phase velocity in the ice, and the presence of electromagnetic contrast between the ice and water. The experimental study of these important parameters was made as follows.

Two 10 mm-diam clear-through parallel holes were melted in sea ice 10 cm from one another by a thermal needle. Metal rods 5 mm in diameter with length exceeding the ice thickness were inserted into the holes. Their lower ends extended beyond the ice-water interface. The metal rods were frozen into the ice, forming a two-conductor "ice" line with wave impedance about 200 Ohms, shorted at the lower boundary of the ice being studied by the sea water. (It was found that the technology used to make the holes does not alter appreciably the ice structure between "ice" line rods.) Then sounding of this line was carried out by video and rf pulses with the aid of a system having a delay line matched with the "ice" line. The pulses were recorded by combined exposure: the pulse reflected from the short circuit in the line made by the operator at the ice-air interface was exposed first, then the short circuit in the air was removed and the pulses were exposed with reflection from the short circuit at the lower end of the "ice" line. Additional gain was not inserted into the circuit in this process.

Comparing the signals reflected from the artificial short circuit at the air-ice interface and from the short circuit formed by the sea water, we can evaluate the overall losses in the "ice" line. These losses are due to absorption in the dielectric (natural sea ice) and by reflection at the air-ice and ice-water interfaces. The latter losses can be considered a measure of the electromagnetic contrast. The measurements were made on perennial pack ice of thickness up to 10 meters, on two-year-old pack ice of thickness from two to three meters, and on young ice one meter thick. These ice types are characterized by different temperature and salinity distribution through the thickness. The experimental values of attenua-

tion as a function of ice thickness are shown in Figure 17. Here the dashed curves are the theoretical curves corresponding to particular specific absorption values.

In spite of the considerable variety of the general physical characteristics of the ices studied, the results of sounding by 25-ns-duration video pulses show that in most cases the specific absorption lies in the range from 0.9 to 2.0 dB/m. The reflectivity can be taken equal to one, otherwise the attenuation curves would cross the abscissa axis above 1.0. This is also valid for 200-MHz-frequency rf pulses and the absorptivity is 4-5 dB/m. Confirmation of the existence of marked electromagnetic contrast at the ice-water interface was also obtained in sounding lines by rf pulses at 400 MHz. However quantitative evaluation at 440 MHz with the line variant is difficult -- reduction of the distance between the "ice" line conductors requires a more complex thermal drilling technique. The results shown here do not indicate precisely what is the reflecting boundary -- the sea water itself or the upper boundary of the layer in which high-concentration brine is present. Radar sounding of an "ice island" was performed to obtain an answer to this question (SP-19 drifting station). Its thickness was 28 - 34 M. Salinity samples were taken from various depths of this "island" and temperature measurements were made. The salinity and temperature values are shown in Table 8.

Since the temperature at depths of 17 meters and below exceeds the eutectic temperature for all the seawater salts, at these depths the liquid phase is present in the body of the flow. Radiosounding of this flow was carried out at 200 MHz by 50 ns duration pulses. The experiments showed that the salinity boundary located at the 17 meter depth yields a strong reflected pulse. The salinity jump at the 19 - 20 meter level also reflects a considerable portion of the sounding pulse energy.

Regular reflection was noted from the ice-water interface. This series of field measurements showed that electromagnetic contrast

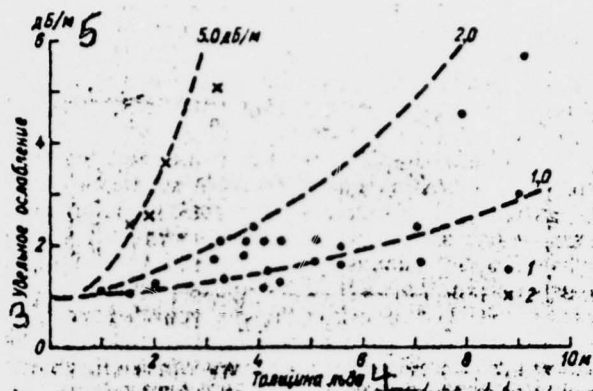


Figure 17. Experimental radio signal specific attenuation as function of ice thickness.
 1- 25 ns duration video pulses; 2- 50 ns duration rf pulses; 3- specific attenuation; 4- ice thickness; 5- dB/m.

arises in ice layers characterized by variation of the salinity, more exactly variation of the liquid phase relative content. Such conditions arise also at the ice-seawater interface. In this connection we should note that the signal which can be considered after reflection from the lower boundary of the ice may begin to form somewhat above this boundary, specifically at the upper boundary of the so-called transition layer. The thickness of this layer is determined by the temperature conditions.

The electromagnetic wave velocity measurements were made using the same technique and the results are shown in Figure 18.

TABLE 8

Sampling depth, m	0-16	17	17.5	18	19	22	32
Salinity, %	0	0.4	0.74	1.47	7.53	8.04	7.98
Temperature, °C	-9	-8.3	-8.3	-7.5	-7.04	-6.0	-1.8

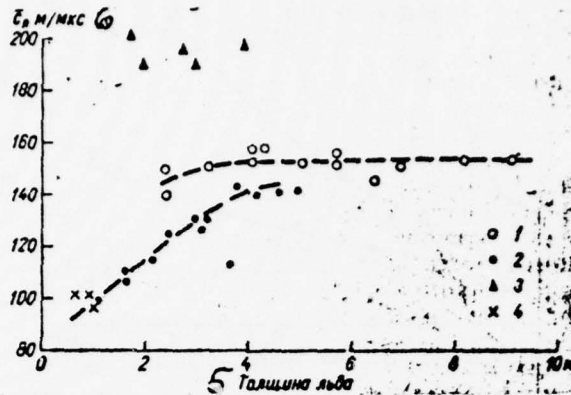


Figure 18. Experimental electromagnetic wave propagation velocity in sea ice as a function of its thickness. 1- in pack ice without snow; 2- in pack ice with snow cover more than 0.5 m thick; 3- in pack ice segment with porous texture; 4- in young ice 1.5 m thick with air temperature from -23°C to 25°C ; 5- ice thickness; 6- m/ μs .

We did not make any special measurements of the electromagnetic characteristics of the ice covers of freshwater bodies. It can be stated a priori that the known results of laboratory measurements made on freshwater ice specimens and also the results of field measurements made on glacier ices can be extended without major error to the ice covers of lakes, rivers, and so on. Here, naturally, we must consider the temperature of these covers and introduce corrections to ϵ' and $\text{tg}\delta$. It should be emphasized that the physical characteristics of freshwater body ice covers are more stable in comparison with the same characteristics for drifting sea ice. The freshwater body ice covers are more uniform through their thickness than the sea ices, there are no salt components in their structure, there is a very marked ice-water crystallization boundary which leads to electromagnetic contrast which is constant and large in magnitude.

Specifics and Techniques of Sea and Freshwater Ice Radiosounding.

The radar measurements made over several years of Antarctic and Arctic glacier thickness have created a good theoretical, procedural, and engineering basis for transition to radiosounding of sea and freshwater ice covers. Several hardware variants [9] have been developed for radiosounding of floating ice thickness. We believe that the pulse radar method is promising for this task. It is simple in technical realization and from the viewpoint of reducing the observational results.

The problem of remote surveying of ice thickness includes obtaining the above-water and under-water relief profiles. The survey scale depends on the carrier vehicle flight altitude, antenna pattern width, and range resolution of the measurement method used. In other words, the specified survey scale defines the radar technical parameters and the aircraft flight conditions. We should also note the influence of factors such as scattering, polarization, and focusing of the waves. Their evaluation is the subject of a separate major study.

We shall indicate some general factors which determine the conditions of floating ice thickness survey with a given scale.

It is well known that the ice surface and under-water relief profiles depend on the age and formation conditions of the ice. Perennial ice has the most uneven surface. The autocorrelation radius L of the outer surface relief of perennial ice is 10 - 15 meters with mean-square deviation σ of the relief heights from the mean surface equal to 0.45 to 0.5 meters. The autocorrelation radius of the under-water relief of perennial ice is about 50 meters. The maximal ice thickness in this radius may reach 12-15 meters with average ice field thickness of four meters. For geophysical purposes it is sufficient to obtain estimates of the thicknesses on an area with radius less than the autocorrelation radius of the outer surface relief. In this case the thickness estimate will be biased, depend-

ing on the surface roughness parameter $(a=2\frac{\sigma}{L})$. For identification of the outer surface relief profile the following condition must be satisfied:

$$\frac{\pi\lambda h_0}{2} \ll \pi L^2,$$

in which the left side is half the area of the first Fresnel zone; h_0 = flight altitude; λ = radar wavelength. For example, for radar carrier frequency 600 MHz resolution of the outer surface relief of ice with autocorrelation radius 10 meters can be obtained with flight altitude less than 400 meters.

We note once again that for fast remote surveying, the method with time separation of the signals reflected from the ice boundaries is more convenient from the technical aspect and in regard to interpretation of the results. The resolution of this method is determined basically by the radiated pulse duration.

Experiments on radiosounding of the Central Arctic drifting sea ice from an airplane were made in the spring of 1973 in the region of the SP-21 drifting station. A pulse radar with the following parameters was selected for the experiments:

Carrier frequency	100 MHz
Pulse duration	50 ns
Antenna directivity	6 dB
Radar potential	140 dB

The radar was located aboard an AN-2 airplane. Flights to measure the thickness were made over the primary ice formations of the Central Arctic; perennial pack fields of thickness more than 3 meters; two-year-old pack of thickness from 2 to 3 meters; and young ice of thickness 1 to 1.5 meter. The measurements were made from 100-m height at 150 km/h air speed. Figure 19 shows the pack ice radar sounding oscilloscopes taken sequentially in time with 0.5 second exposure. The time delay between the pulses reflected from

the upper and lower boundaries of the ice are clearly seen on the right side of the oscilograms. The distance between their peaks indicates the pack ice thickness to some definite scale.

A characteristic feature of the reflected pulses received aboard the airplane is their short "lifetime," i.e., the low temporal stability of the image. The lifetime is determined by the carrier airplane flight speed and certain other factors. The levels of the reflected signals recorded in flight are determined by the state of the reflecting surfaces and by the physical characteristics of the ice. Relief irregularity and different degree of conformance of the snow cover and the upper ice layers lead to fluctuations of the signal reflected from the upper surface of the ice. These same factors together with scattering and absorption within the ice, which have spatial variability, lead to fluctuations during flight of the signals reflected from the lower surface of the ice.

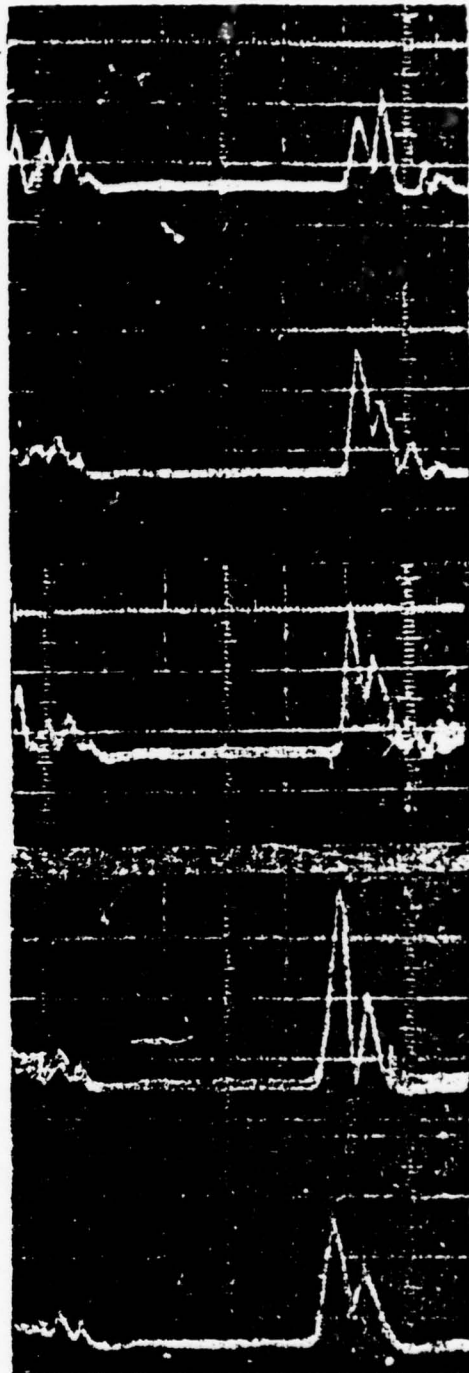


Figure 19. Pack ice sounding oscilloscopes.

The size of the area illuminated by the radar also influences the nature of the fluctuations. Signal fluctuations are also observed when sounding young ice fields with smooth boundary surfaces, although these fluctuations are weaker.

The measurements showed that the overall attenuation of the signals reflected by the upper surface of the ice during flight above pack ice at 100 meters altitude varies in the range from 90 to 120 dB. The theoretical geometric losses are 80 dB, the losses caused by reflection (Fresnel) for $\epsilon_r = 3.5$ are 10 dB, the losses resulting from surface scattering and media impedance mismatch do not exceed 30 dB (for young ice the latter does not exceed 10 dB). The overall attenuation of the signals reflected by the lower surface of the ice is approximately the same order of magnitude. In Figure 20 the dashed lines are the theoretical curves of overall attenuation of the signal reflected from the lower surface versus ice thickness for fixed values of the specific absorption in homogeneous ice with plane-parallel boundaries. The points are the experimental signal attenuation values. We see from the figure that the specific absorption does not exceed 1-5 dB/m for this series of studies, conducted above the most characteristic Central Arctic ices in April, 1973. The entire range of recorded signal amplitudes is shown in Figure 20. The signals shown in Figure 19 were recorded with exposure time 0.5 sec; during this time the carrier vehicle traveled 20 meters. Therefore it seems probable that statistical interpretation of the measurement results will be very promising in the future. This requires photographic recording of the reflected signals with short exposure time or with the aid of a high-speed storage system.

These summertime experiments uncovered still another important problem of ice sounding; namely, the reliability of the electromagnetic wave velocities in the ice. It is well known that the electromagnetic wave velocity in sea ice is determined by the relative content of the liquid, solid, and gaseous phases. In other words, the radio signal velocity will be different in ices of different age and ice formation conditions. Measurements were made of the thickness-

BEST AVAILABLE COPY

average velocity of vertical electromagnetic wave propagation in the ice fields located along the flight paths. The measurements showed that the wave velocity has different values in the same pack field. On the snow-free areas the velocity was on the average 150 m/ μ sec, on areas where the snow cover exceeds thickness 0.5 meter the velocity is much lower and decreases with reduction of the ice thickness. Because of this the radar sounding data will

make the pack field appear more homogeneous in thickness than it actually is. In slush zones, where the ice has a porous texture, the wave velocity is 190 - 300 m/ μ sec, the wave velocity in one-meter-thick young ice with stable air temperature of -23, -25°C is 90 - 100 m/ μ sec. We can expect that the rf signal velocity in young ice will also be determined to considerable degree by the ice temperature regime. The velocity will be lower, the thinner the ice and the higher its temperature. The marked variability of signal propagation velocity in sea ice requires for correct interpretation of the radar thickness survey classification of the ices being sounded and account for the thickness of the snow cover and the temperatures of the ice and of the snow cover.

In conclusion we note that the series of studies made by Tripol'nikov on Central Arctic drifting ice enriched considerably our knowledge of the electromagnetic characteristics of the primary drifting ice forms. These measurements created the physical basis for radiosounding of sea ice cover and in some measure, freshwater ice cover. The remote measurements of drifting ice thickness from an airplane confirmed the fundamental possibility of recording sea ice thickness using the pulse radar method. Analysis of these

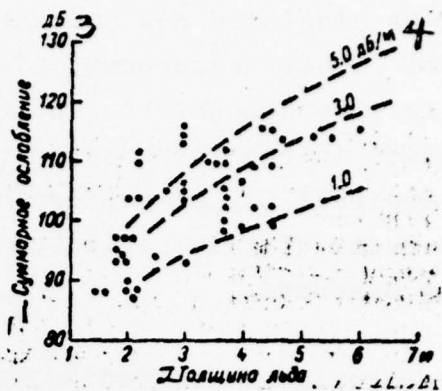


Figure 20. Overall attenuation of radio signal during airplane sounding of drifting ice of different thickness. 1- overall attenuation; 2- ice thickness; 3- dB; 4- dB/m.

experiments disclosed new and very important aspects of the general problem of remote measurement of sea ice cover thickness: the need for taking into account the influence of snow cover and temperature distribution in the ice body on radio signal propagation velocity, and the desirability of performing statistical analysis of the recorded radio signals reflected by the bounding surfaces of the ice being measured.

The experiments on radiosounding of freshwater body ice covers will probably differ somewhat from those discussed above. Specifically, the lower absorption of rf waves in the ice and the higher stability of the electromagnetic wave propagation velocity in the interior of freshwater ice will have an effect. On the other hand, the high (in comparison with sea ice) electromagnetic wave velocity in freshwater ice makes it necessary to increase the radar resolution in order to measure freshwater and sea ices which are comparable in thickness. Remote stationary measurements of lake ice about two meters thick were discussed in [21].* Radiosounding was performed at three frequencies: 10^4 , 10^3 , and 440 MHz, the pulse durations were 15, 25 and 25 ns respectively. The experiments showed that there is reliable indication of the pulses from the upper and lower surfaces of ice covers which are snow covered and those which are free of snow. These experiments confirm convincingly the promising nature of radar sounding of freshwater ice.

10. APPLICATION OF THE PULSE RADAR METHOD IN OTHER GEOPHYSICAL OPERATIONS

The theoretical questions examined above relative to electromagnetic wave propagation in various ices and their experimental resolution are a serious prerequisite for successful solution of the problem of radar sounding of other media: permafrost, desert sands to detect aquifer strata, and also fresh water. The experience

* Radiosounding was conducted by installations located on the ice.

accumulated in sounding ices and the widespread use of various equipment for this purpose makes it possible to examine the questions of the methods and techniques for sounding these media.

Electrical Properties of Permafrost, Sands, and Fresh Water in the rf Band.

At the present time permafrost properties have been studied most completely using direct current [15]. The data available on permafrost properties at the radio frequencies [15] do not provide a picture of their variability as functions of electromagnetic field frequency or permafrost structure and condition. Because of this we conducted studies of the electrical properties of permafrost materials on specimens obtained from certain regions of the Soviet Arctic [26].

Data on the electrical properties of sand with varying water content in the 3-30 MHz frequency range, obtained at AANII, are presented in [14].

An important result of these measurements is the fact that the electrical properties of dry sand at 30 MHz ($\epsilon' = 3$, $N = 0.104$ dB/m) are practically identical to the properties of fresh water at -1°C [14]. We would expect that under natural conditions the properties of dry sand would be similar to those measured under laboratory conditions while the properties of wet sand may differ considerably, particularly with the presence of dissolved salts.

The electrical properties of fresh water have been studied by several authors [4, 23]; however the data obtained (without indication of the chemical composition of the water) differ markedly. This drawback was taken into consideration in our measurements, made in Lakes Gladyshevskoye (Karelian Isthmus) and Onezhskoye. On the basis of our measurements we can consider that ϵ' of lake water in the meter band is about 81 and varies somewhat with temperature change. In this same band the absorptivity is about 1.5 - 2 dB/m.

In analyzing the electrical properties of permafrost, sand, and fresh water we can note the following:

1. the dielectric permeability of these media does not vary significantly in the frequency band above 10 MHz, i.e., in this band these media do not have significant dispersion;

2. the absorptivity in the 10-30 MHz band ranges from 0.03 to 2 dB/m, sometimes reaching (for permafrost) 10 dB/m. In all these media absorption increases with increase of the frequency.

The absence of dispersion and the comparatively low absorptivity make it possible to select a frequency band which is promising for the sounding of permafrost, sand, and fresh water. This band includes the 10-30 MHz frequencies. In certain cases, when the absorption is low, higher frequencies up to 200-300 MHz can be used.

Calculation of Overall rf Signal Attenuation in Layers of Permafrost, Sand, and Fresh Water.

The overall attenuation calculation presented in Section 5 can be used to determine the signal levels in vertical sounding of other media. The values of the individual attenuation components were obtained by Trepov. We shall present their values:

- signal attenuation due to focusing N_f for $h_0 \ll h$ is -5 dB for sand; -6 dB to -9 dB for permafrost, and -19 dB for water;

- the scattering N_p by the surface of the medium is determined by the Fresnel coefficient of the air-medium interface and constitutes for passage in both directions 0.7 dB for sand, 0.9 to 2.5 dB for permafrost, and 8.8 dB for water;

- the losses N_{dep} , caused by signal depolarization are not known and are subject to study; in many cases they may be very low;

- the losses N_{tot} are determined by the Fresnel coefficient of the interface of the medium being sounded and the underlying medium. For the calculation we can take the following conditions at the lower boundary:

1. Reflection in sand takes place from the surface of water concentration change from 0.1 ($\epsilon' = 4$ for $f = 30$ MHz) to 0.2 ($\epsilon' = 10$). Here $K_f = 0.228$, $N_{\text{tot}} = 12.8$ dB.

2. For permafrost N_{tot} varies from 24.6 dB (for permafrost with $\epsilon' = 8$) to 19 dB (for permafrost with $\epsilon' = 4$). In the calculation it was assumed that the underlying formation is wet sand ($\epsilon' = 10$ at 30 MHz).

3. When sounding a freshwater basin the losses (N_{tot}) at the water-bottom interface are 5.6 dB for rocky bottom ($\epsilon' = 8$), for sandy bottom with water concentration in the sand 0.38 ($\epsilon' = 27.5$ for $f = 30$ MHz) $N_{\text{tot}} = 11.6$ dB). Table 9 presents rf signal absorptivity in the media for which the intrascopy problem is discussed in the present study.

The final expressions for the overall losses (in dB) for $\lambda=10$ m, $G=2$, $h_0 \rightarrow 0$ have the form:

1. for sand $N_z = N_{\text{sh}} + 20 \lg h + 11.1$
2. for permafrost $N_z = N_{\text{sh}} + 20 \lg h + 14.5$
3. for water $N_z = N_{\text{sh}} + 20 \lg h + 3.8$

Region of Application of Radar Sounding of Sands, Permafrost, and Fresh Water.

On the basis of the above overall attenuation calculation, assuming a radar potential for example of 160 - 170 dB, we can evaluate the sounded layer thickness for which the reflected signal exceeds the receiving channel noise level. These data are presented in Table 10 and were calculated with the antennas located in the air near

TABLE 9
AVERAGED ELECTRICAL CHARACTERISTICS OF SOME MEDIA

Medium	Velocity, m/ μ s	Absorptivity at 30 MHz, dB/m
Cold glaciers	167	0.02-0.03
Warm and temperature glaciers	167	0.06-0.08
Permafrost	110	1.5-5.0
Freshwater bodies	33	1.0-2.0
Sandy soil:		
- dry	113	1.5-2.0
- wet	55	
Pack Sea Ice	150	1-2
Young Sea Ice	100	3-6

the upper surface of the medium (except for water).

Technique and Procedural Characteristics of Radar Sounding of
Strongly Absorbing Media.

If we consider the primary objective of radar sounding of media to be the measurement of the thickness of their layer to the boundaries with the underlying formations or to the temperature jump surfaces, then by analogy with glacier sounding we can identify three types of problems, the technique and procedure for the solution of which differ:

1. measurement of the maximal layer thicknesses;
2. measurement of thicknesses which are definitely less than the maximal thicknesses measurable with the aid of radar sounding;
3. measurement of small thicknesses, for example the freezing depth of soil or of thin layers of sand and water.

TABLE 10
THICKNESS OF SOUNDED LAYER FOR SOME MEDIA
(RADAR POTENTIAL 160 - 170 dB)

MEDIUM	RADAR CARRIER FREQUENCY, MHz	ICE THICKNESS, M
Dry Sand	30	600
Wet Sand:		
- Water concentration 0.1 g/g	30	140
- Without salts 0.2 g/g	30	40
Rock-ice permafrost ($t=-15^{\circ}\text{C}$)	10	250
Frozen soil	10	15
Fresh water:		
- from [17]	30	100
- from [4]	30	3000

The selection of equipment parameters such as carrier frequency, radiated power, frequency spectrum width (pulse duration for pulse radars), and processing in the receiver do not present any difficulty. Typical parameters of the radar for measuring the maximal thickness of permafrost, sand, and fresh water may be as follows:

Carrier frequency	10 MHz
Pulse power	100 kW
Pulse duration	0.3 μs
Receiver bandwidth	3 MHz
Radar potential	183 dB

The parameters of the radar for solving problems of the second type may be as follows:

Carrier frequency	30 MHz
Pulse power	10 kW
Pulse duration	0.1 μs
Receiver bandwidth	15 MHz
Radar potential	165 dB

Typical parameters of the radar for measuring thin layers of permafrost, sand, and water are:

Carrier frequency	150 MHz
Pulse power	100 W
Pulse duration	0.015 μ s
Receiver bandwidth	70 MHz
Antennas	wideband
Radar potential	120 dB

In spite of the fact that radar sounding of the considered media is possible and suitable apparatus can be developed, in the practical application of the method there are several serious difficulties:

1. The high noise level in the form of reflections from irregularities on the surface of the medium and nonhomogeneities within the medium may make it difficult to identify and interpret the useful signal;

2. Noise in the form of direct signal transmission from the transmitter output to the receiver input and reflections from the surface increase the minimal measurable thickness. Considering that the absolute delay time for the maximal measurable thickness is short (2 to 10 μ s), the thickness range which can be measured in practice may be too small.

We shall not discuss the special procedural and hardware techniques which can be used to eliminate these problems. We shall show that two of the problems posed above, namely radiosounding of fresh water and sand, have been resolved experimentally.

First Experiments on Radar Sounding of Fresh Water and Sand.

The first radar sounding of fresh water was accomplished in Lake Gladyshevskoe in August 1969. A pulse radar fabricated by Radiophysics Division of AANII was used for sounding. Its specifications were:

Carrier frequency	45 MHz
Pulse power	1 W
Pulse duration	0.1 μ s
Pulse repetition frequency	100 Hz
Receiver passband	10 MHz
Potential	110 dB

The receiving and transmitting antennas -- halfwave dipoles with reflectors in the form of metal sheets -- were submerged in the water. In the sounding process we recorded the signals from an artificial reflector (metal sheet) and from the bottom of the lake for various depths up to the maximal depth for this particular lake of 15 meters. The lake bottom consisted of sand, mud, and rocky strata.

The experiments with the artificial reflector made it possible to determine the radio pulse velocity in the water; it was 33.3 m/ μ s ($\epsilon' = 81$). We also obtained from the sounding results the specific attenuation of the radio signal; for this particular body of water N_u was equal to 1.4 dB/m.

In 1971 studies were made in the Petrozavodsk Inlet of Lake Onezhskoye. In these experiments we used a more powerful radar with carrier frequency 60 MHz and pulse duration 0.4 μ sec. The radio-sounding was conducted with ship speed about 10 km/h. The antennas were submerged in the water. The radio pulse propagation velocity in this lake was 33 m/ μ sec ($\epsilon' = 82.6$) with water temperature 10°C. The specific absorption was different on the different tacks: 2 and 1.75 dB/m. High values of the specific resistance (2 dB/m) were obtained on tacks passing near urban sewer outfalls. It was noted that the different geological materials forming the bottom have different reflectivity. The values of $\text{tg}\delta$ were calculated from the experimental data for the waters of Lakes Onezhskoye and Gladyshevskoye and compared with the results of laboratory measurements performed by Saxton and other investigators. Radiosounding of Lakes Gladyshevskoye and Onezhskoye shows that the radar method makes it possible to measure comparatively simple the depth of fresh water bodies,

detect objects in the water, determine the electrical properties of the water under natural conditions, and evaluate the degree of contamination of water bodies.

In July 1972 radiosounding of gravelly sand was carried out by the Valdai Scientific Research Hydrological Laboratory of the State Hydrological Institute in order to determine groundwater depth. According to hydrological observation data groundwater lies at depths of 6.7 and 13 meters in the regions studied. Sounding was performed with a radar with the following characteristics:

Carrier frequency	60 MHz
Pulse duration	0.1 μ s
Radiated power	1 kW
Potential	150 dB

Several series of radiosoundings were conducted, differing in mutual positioning of the receiving and transmitting antennas (half-wave dipoles), field polarization, and distance between the antennas. To facilitate interpretation of the received signals the antennas were positioned in the upper layer of the sand at depths from 0.1 to 0.4 meters. We also used reflectors in the form of sheets and tubes positioned on the sand surface above the antennas. The experiments disclosed the presence of four characteristic signals: direct signal from antenna to antenna, traveling through the air; direct signal from antenna to antenna, traveling in the ground; signal scattered by the upper surface of the water-saturated layer; and in certain cases the signal scattered by the lower surface of this layer. Analysis of the oscillograms showed that in the region with the aquifer layer located at a depth of 6.7 m the signal reflected from the layer lying at the 7 m depth is noted: the layer thickness was about 3 m. In the second case, when the layer was located at a depth of 13 m, radiosounding also showed this depth, i.e., 13 m. The thickness of the water-saturated layer from the radiosounding data was 11 m in this case.

This sounding investigation is believed to be the first experimental proof of the feasibility of searching for and locating groundwater with the use of radar techniques.

REFERENCES

1. Avsyuk, G. A. Glacier Temperatures. Izv. AN SSSR, Ser. geogr. No. 1, 1955, pp. 14-31.
2. Atlas Antarktiki (Atlas of Antarctica). Vol. 1, Leningrad, Izd. GUGK, SSSR, 1966, 66 pgs.
3. Bogoroditskiy, N. P. Teoriya dielektrikov (Theory of Dielectrics). Moscow-Leningrad, Energiya Press, 1965, 344 pgs.
4. Bogoroditskiy, N. P. and V. V. Pasylkov, Materialy v radio-elektronike (Materials in Radioelectronics). Moscow, Gosenergoizdat Press, 1965, 346 pgs.
5. Bogoroditskiy, V. V. Fizicheskiye issledovaniya lednikov (Physical Studies of Glaciers). Leningrad, Gidrometeoizdat Press, 1968, 214 pgs.
6. Bogorodskiy, V. V., L. S. Govorukha and B. A. Fedorov, Some Results of Radar Sounding of Arctic Glaciers. Tr. AANII, Vol. 294, 1970, pp. 87-93.
7. Bogorodskiy, V. V. and V. N. Rudakov, Electromagnetic Methods of Determining Floating Ice Thickness. Zhurn. tekhn. fiziki, Vol. 32, No. 7, 1962, pp. 874-882.
8. Bogorodskiy, V. V. and G. V. Trepov, Radar Measurement of Mountain Glacier Thickness. Zhurn. tekhn. fiziki, Vol. 38, No. 8, 1968, pp. 1389-1391.
9. Bogorodskiy, V. V. and V. P. Tripol'nikov, Radar Survey of Floating Ice Cover Thickness. Problemy Arktiki i Antarktiki, No. 39, 1972, pp. 135-137.
10. Bogorodskiy, V. V. and B. A. Fedorov, Radar Survey of Glaciers, Zhurn. tekhn. fiziki, Vol. 37, No. 4, 1967, pp. 781-788.
11. Bogorodskiy, V. V. and B. A. Fedorov, Radar Sounding of Severnaya Zemlya Glaciers. Tr. AANII, Vol. 295, 1970, pp. 5-16.
12. Bogorodskiy, V. V. and G. P. Khokhlov, Electrical Characteristics of Drifting Sea Ice in the 100 Hz to 1 MHz Band. DAN SSSR, Vol. 189, No. 6, 1969, pp. 1230-1232.

13. Finkel'shteyn, M. I., V. G. Glushnev, A. I. Petrov, V. Ya. Ivashchenko, Anistropy of Radiowave Attenuation in Sea Ice. Izv. AN SSSR, ser fizika atmosfery i okeana, Vol. 6, No. 3, 1970, pp. 311-313.
14. Bogorodskiy, V. V., G. V. Trepov, B. A. Fedorov, and G. P. Khokhlov, On the Possibility of Radar Sounding of Sand for the Detection of Aquifer Strata. Izv. AN SSST, ser fizika zemli, No. 7, 1973, pp. 119-120.
15. Parkhomenko, E. I. Elektricheskiye svoystva gornykh porod (Electrical Properties of Rocks). Nauka Press, Moscow, 1965, 168 pgs.
16. Pustyl'nik, Ye. I. Statisticheskiye metody analiza i obrabotki nablyudeniy (Statistical Methods of Analysis and Reduction of Observations). Nauka Press, Moscow, 1968, 288 pgs.
17. Bogorodskiy, V. V., G. V. Trepov, B. A. Fedorov and G. P. Khokhlov, Radar Sounding of Fresh Water. Tr. AANII, Vol. 295, 1970, pp. 185-187.
18. Rudakov, V. I. and V. V. Bogorodskiy, Measurement of Glacier Thickness by Electromagnetic Methods. Zhurn. tekhn. fiziki, Vol. 30, No. 1, 1960, pp. 82-89.
19. Sovolev, V. V. Perenos luchistoy energii v atmosferakh zvezd i planet (Radiant Energy Transport in Planet and Star Atmospheres). Nauka Press, Moscow, 1956, 391 pgs.
20. Trepov, G. V. Measurement of Electromagnetic Wave Propagation Velocity in a Glacier. Tr AANII, Vol. 295, 1970, pp. 60-63.
21. Finkel'shteyn, M. I., V. G. Glushiyev and A. N. Petrov, Radar Sounding of Lake Ice. Izv. AN SSST, ser fizika atmosfery i okeana, Vol. 7, No. 112, 1971, pp. 1323-1325.
22. Frolich, G., Teoriya dielektrikov (Theory of Dielectrics). Moscow, IL, 1960, 249 pgs.
23. Von Hippel, A. R., Dielektriki i ikh primeneniye (Dielectric Materials and Applications). Moscow, Gosenergoizdat Press, 1959, 438 pgs.
24. Tsukernik, V. B., A. I. Frolov and P. A. Stroyev, Seismic and Gravimetric Studies on the West Shelf Glacier in Antarctica. Izv. AN SSSR, ser. geofiz., No. 6, 1963, pp. 907-921.

25. Shumskiy, P. A., Osnovy strukturnogo ledovedeniya (Fundamentals of Structural Glaciology). Moscow, Izd-vo AN SSSR, 1965, 492 pgs.
26. Bogorodskiy, V. V., G. V. Trepov, B. A. Fedorov and G. P. Khokhlov, Electrical Properties of Permafrost Formations and Radiowave Attenuation Therein. Izv. AN SSSR, ser. fizika zemli, No. 6, 1971, pp. 86-88.
27. Bogorodskiy, V. V., G. P. Khokhlov, B. A. Fedorov and G. V. Trepov, Electrical Characteristics of Rock-Ice Systems, DAN SSSR, Vol. 190, No. 1, 1970, pp. 88-90.
28. Addison, J. K. Electrical Properties of Saline Ice. J. Appl. Physics, Vol. 40, No. 8, 1969, pp. 3105-3114.
29. Cook, I. C. RF-Electrical Properties of Salty Ice and Frozen Earth, J. Geophys., Vol. 65, No. 6, 1960, pp. 1767-1771.
30. Fujino, K. Electrical Properties of Sea Ice. Physics of Snow and Ice. Intern. conf. low temperatures. The Univ. Hokkaido, Vol. 1, t. 1, 1967, pp. 633-648.
31. Jiracek, G. R. Radiosounding of Antarctic Ice. Univ. Wisconsin Geophys. and Polar Research Center, 1967, p. 127.